



## Co2 chemisorption by functionalized amino acid derivatives.

Fehrmann, Rasmus; Riisager, Anders; Shunmugavel, Saravanamurugan

*Publication date:*  
2015

*Document Version*  
Publisher's PDF, also known as Version of record

[Link back to DTU Orbit](#)

*Citation (APA):*  
Fehrmann, R., Riisager, A., & Shunmugavel, S. (2015). Co2 chemisorption by functionalized amino acid derivatives. (Patent No. WO2015107060).

---

### General rights

Copyright and moral rights for the publications made accessible in the public portal are retained by the authors and/or other copyright owners and it is a condition of accessing publications that users recognise and abide by the legal requirements associated with these rights.

- Users may download and print one copy of any publication from the public portal for the purpose of private study or research.
- You may not further distribute the material or use it for any profit-making activity or commercial gain
- You may freely distribute the URL identifying the publication in the public portal

If you believe that this document breaches copyright please contact us providing details, and we will remove access to the work immediately and investigate your claim.

(51) International Patent Classification:  
*B01D 53/14* (2006.01)(21) International Application Number:  
PCT/EP2015/050546(22) International Filing Date:  
14 January 2015 (14.01.2015)

(25) Filing Language: English

(26) Publication Language: English

(30) Priority Data:  
14151289.7 15 January 2014 (15.01.2014) EP(71) Applicant: **DANMARKS TEKNISKE UNIVERSITET**  
[DK/DK]; Anker Engelunds Vej 1, DK-2800 Kgs. Lyngby (DK).(72) Inventors: **FEHRMANN, Rasmus**; Eckersbergsgade 23, DK-2100 Copenhagen Ø (DK). **RIISAGER, Anders**; Rønnevangshusene 138, DK-2630 Taastrup (DK). **SHUN-MUGAVEL, Saravanamurugan**; Skovfryd 6, DK-2800 Kgs. Lyngby (DK).(74) Agent: **ZACCO DENMARK A/S**; Arne Jacobsens Allé 15, DK-2300 Copenhagen S (DK).

(81) Designated States (unless otherwise indicated, for every kind of national protection available): AE, AG, AL, AM, AO, AT, AU, AZ, BA, BB, BG, BH, BN, BR, BW, BY, BZ, CA, CH, CL, CN, CO, CR, CU, CZ, DE, DK, DM, DO, DZ, EC, EE, EG, ES, FI, GB, GD, GE, GH, GM, GT, HN, HR, HU, ID, IL, IN, IR, IS, JP, KE, KG, KN, KP, KR, KZ, LA, LC, LK, LR, LS, LU, LY, MA, MD, ME, MG, MK, MN, MW, MX, MY, MZ, NA, NG, NI, NO, NZ, OM, PA, PE, PG, PH, PL, PT, QA, RO, RS, RU, RW, SA, SC, SD, SE, SG, SK, SL, SM, ST, SV, SY, TH, TJ, TM, TN, TR, TT, TZ, UA, UG, US, UZ, VC, VN, ZA, ZM, ZW.

(84) Designated States (unless otherwise indicated, for every kind of regional protection available): ARIPO (BW, GH, GM, KE, LR, LS, MW, MZ, NA, RW, SD, SL, ST, SZ, TZ, UG, ZM, ZW), Eurasian (AM, AZ, BY, KG, KZ, RU, TJ, TM), European (AL, AT, BE, BG, CH, CY, CZ, DE, DK, EE, ES, FI, FR, GB, GR, HR, HU, IE, IS, IT, LT, LU, LV, MC, MK, MT, NL, NO, PL, PT, RO, RS, SE, SI, SK, SM, TR), OAPI (BF, BJ, CF, CG, CI, CM, GA, GN, GQ, GW, KM, ML, MR, NE, SN, TD, TG).

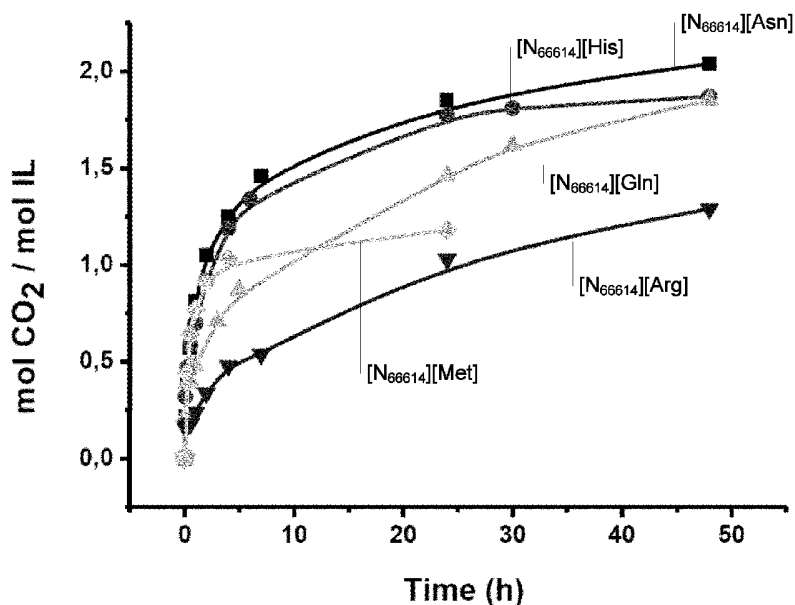
Published:  
— with international search report (Art. 21(3))(54) Title: CO<sub>2</sub> CHEMOSORPTION BY FUNCTIONALIZED AMINO ACID DERIVATIVES(57) Abstract: The absorption and desorption behaviour of carbon dioxide (CO<sub>2</sub>) using a composition comprising an ionic compound comprising a cation [A<sup>+</sup>] and an anion [B<sup>-</sup>] is described, wherein the anion [B<sup>-</sup>] is a mono-amine functionalized amino acid.

Fig. 1

## CO<sub>2</sub> chemisorption by functionalized amino acid derivatives

### Field of the invention

The present invention concerns the absorption and desorption behaviour of carbon  
5 dioxide (CO<sub>2</sub>) using mono-amine functionalized amino acids.

### Background of the invention

Carbon dioxide is recognized as a greenhouse gas that contributes to climate  
changes. A major cause of CO<sub>2</sub> emission is from combustion of fossil fuels like oil and  
10 coal in production of electricity and heat. The world consumption of coal is expected to  
increase by 49% in 2030 and accordingly much attention has been focused on  
reducing CO<sub>2</sub> emission from power plant flue-gas streams. Currently, aqueous  
solutions of organic amines are being used to capture CO<sub>2</sub> in scrubbers as  
carbamates despite concerns about, e.g. low absorbent capacity and energy intensive  
15 regeneration by desorption, which may require up to one-third of the total energy  
output from the power plant. Other technical challenges with amine sorbents include  
corrosion of steel pipes and pumps as well as thermal and chemical decomposition. In  
addition concern has been expressed about emission of the amines to the atmosphere  
leading to serious human health hazards. Solid absorbers also work unsatisfactorily  
20 among others due to the high desorption energy required to desorb CO<sub>2</sub> and  
regenerate the absorber.

In order to overcome these inherent problems, it is highly desired to develop a viable  
and energy-efficient technology for CO<sub>2</sub> capture by use of alternative, suitable  
25 absorbents.

Ionic liquids (ILs) are promising candidates as absorbents in CO<sub>2</sub> removal due to their  
relatively high thermal stability, exceptionally low vapour pressure and tuneable  
physicochemical properties [see eg. F. Jutz et al. *Chem. Rev.* 2011, 111, 322; and J.  
30 Huang et al. *Aust. J. Chem.* 2009, 62, 298]. There have been many reports on CO<sub>2</sub>  
capture using common ILs (typically referred to as first-generation ionic liquids), and a  
maximum CO<sub>2</sub> absorption capacity of 0.75 in mole fraction of CO<sub>2</sub> has been found for  
[C<sub>8</sub>MIM][PF<sub>6</sub>] (1-methyl-3-octylimidazolium hexafluorophosphate) at 40°C under 93 bar  
pressure [see eg. L.A. Blanchard, Z. Gu, Joan F. Brennecke, *J. Phys. Chem. B* 2001,  
35 105, 2437; Z. Gu, Joan F. Brennecke, *J. Chem. Eng. Data* 2002, 47, 339; and Sudhir

N. V. K. Aki, Berlyn R. Mellein, Eric M. Saurer, Joan F. Brennecke, *J. Phys. Chem. B* 2004, 108, 20355]. The CO<sub>2</sub> absorption capacity of these kinds of ILs is, however, limited due to the relatively weak physisorption taking place between the IL and CO<sub>2</sub>. To circumvent this drawback, Davis and co-workers developed task-specific ionic liquids (TSILs) which are able to chemically bind CO<sub>2</sub> to amine-functionalised imidazolium-based IL at ambient conditions. Even though these TSILs form a chemical bond with CO<sub>2</sub> the absorption capacity was only 0.5 mol of CO<sub>2</sub> per mol of IL (mole ratio of 0.33) due to intermolecular carbamate formation (i.e. a 1:2 mechanism) [see Eleanor D. Bates et al., *J. Am. Chem. Soc.* 2002, 124, 926].

Zhang et al. have proposed a new mechanism for the formation of carbamic acid after CO<sub>2</sub> absorption in phosphonium-based amino acid functionalised ILs [J. Zhang, S. Zhang, K. Dong, Y. Zhang, Y. Shen, X. Lv. *Chem. Eur. J.* 2006, 12, 4021]. In this mechanism, one mol of CO<sub>2</sub> also reacted with two moles of IL. However in presence of water (1 wt.%), the IL could absorb an equimolar amount of CO<sub>2</sub> via a bicarbonate mechanism (mole ratio of 0.5). Recently, the formation of carbamic acid in amino acid-based ILs was further confirmed by Brennecke and co-workers by examining proline and methionine functionalised phosphonium-based ILs for CO<sub>2</sub> absorption. Here it was shown that one mol of IL can absorb one mol of CO<sub>2</sub> (1:1 mechanism) [see B. E. Gurkan, J. C. de la Fuente, E. M. Mindrup, L. E. Ficke, B. F. Goodrich, E. A. Price, W. F. Schneider, J. F. Brennecke, *J. Am. Chem. Soc.* 2010, 132, 2116]. A few other reports have also published equimolar amount of CO<sub>2</sub> absorption in functionalised ILs, but the typical CO<sub>2</sub>-absorption capacity for published IL based solutions is sub-stoichiometric rather than super-stoichiometric.

Chemical absorption (chemisorption) of CO<sub>2</sub> was first observed in imidazolium acetates, where the CO<sub>2</sub> can be trapped either as bicarbonate or, as recently found, also as a carboxylate on carbon position 2 of the imidazole via a carbene mechanism [US 10/737,090; US 5,336,298; Maginn, E., DOE Report, quarterly, 01/05- 03/05 2005, 1–12, DOE Scientific and Technical Information, Oak Ridge, TN]. This was recently proven by Rogers and co-workers upon determination of its crystal structure [Gurau G et al. *Angew Chem Int Ed*, 2011, 50:12024–12026]. However, amine functionalized ILs have proven to have a higher CO<sub>2</sub> uptake stoichiometry and has attracted more attention.

If an amine functionality is linked to the cation, intermolecular carbamate formation takes place resulting in a maximum stoichiometry of 0.5 moles of CO<sub>2</sub> per mol of IL

[Galan Sanchez L et al., *Solvent properties of functionalized ionic liquids for CO<sub>2</sub> absorption*, Chem Engineer Res Design, 2007, 85: 31–39; and Soutullo M et al.,

5 *Reversible CO<sub>2</sub> capture by unexpected plastic-, resin-, and gel-like ionic soft materials was discovered during the combi-click generation of a TSIL library*, Chem Mater, 2007, 19: 3581–3583]. This has been demonstrated for imidazolium-based cations, where the amine is introduced on one of the alkyl chains. A major drawback of this method is that the already high viscosity of the IL becomes much higher when attaching another  
10 functional group to the IL. The important point is, however, that these compounds show much higher CO<sub>2</sub> uptake than their non-functionalized counterparts.

If the amine functionality is attached to the anion of the IL, carbamate species also form, but there is a possibility that the negatively charged functionality on the anion

15 can take up the proton released upon CO<sub>2</sub> capture forming carbamic acid. Then CO<sub>2</sub> can be absorbed with a stoichiometry of up to 1:1, meaning much more efficient use of the IL. However, in most cases, the absorption capacity still corresponds to 0.5:1. This could very well be related to residual water in the IL interfering with the released proton, preventing it from protonating the anionic part.

20 Therefore it must be concluded that despite growing demand, there has not yet been suggested a satisfactory and economically feasible technical solution to the problem of removing CO<sub>2</sub> from e.g. flue gases which has a high sorption efficiency, a high capacity and a sufficient robustness to allow for uninterrupted performance over long  
25 time periods.

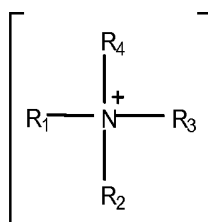
### Summary of the invention

It has surprisingly been found that compositions comprising ionic liquids (ILs) based on simple tetraalkylammonium salts of amine functionalized amino acids are excellent

30 absorbers of CO<sub>2</sub> having high sorption efficiencies. In particular it has been found that super-stoichiometric absorption of high amounts of CO<sub>2</sub> at ambient temperature and pressure (i.e. 2 mol CO<sub>2</sub> per mol IL) is observed for specific compositions. The IL may be adsorbed on a porous (including mesoporous) material.

In a **first aspect** the present invention therefore provides a composition for absorption/desorption of gaseous carbon dioxide (CO<sub>2</sub>), the composition comprising an ionic compound comprising a cation [A<sup>+</sup>] and an anion [B<sup>-</sup>], wherein the anion [B<sup>-</sup>] is a mono-amine functionalized amino acid and the cation [A<sup>+</sup>] is given by the formula:

5



wherein R<sub>1</sub> is a C<sub>n</sub> alkyl chain where n is an integer having a value of at least 10 and not more than 30, and R<sub>2</sub>, R<sub>3</sub> and R<sub>4</sub> are individually selected from the group of methyl, ethyl, propyl, butyl, pentyl, hexyl, heptyl and octyl.

10

By the above is obtained an absorption of CO<sub>2</sub> gas at ambient conditions corresponding to unprecedented 2.0 ± 0.1 mol of CO<sub>2</sub> per mol of IL. This is significantly higher than previous observed results.

15

At elevated temperature, the absorption capacity of the composition is observed to drop to 1 mol CO<sub>2</sub> per mol of IL, demonstrating that it is possible to desorb the CO<sub>2</sub> gas under CO<sub>2</sub>-rich conditions by temperature-swing absorption. By changing the temperature and/or pressure and keeping the composition at these conditions for a longer period of time, it is possible to desorb all the absorbed CO<sub>2</sub>. Moreover, an improved performance after a first cycle in consecutive sorption cycles is advantageously observed by the composition according to the first aspect of the invention.

20

By the composition according to the first aspect of the invention, formation of carbamic acids by reaction of CO<sub>2</sub> with the amine groups according to a 2:1 mechanism is obtainable.

25

In a **second aspect** the invention provides a method for absorption of gaseous CO<sub>2</sub> from a gas stream, the method comprising contacting said gas stream with a composition according to the **first aspect** of the invention.

30

In a **third aspect** the invention also provides a method for desorption of the absorbed CO<sub>2</sub> absorbed on a composition according to the **first aspect** of the invention, the method comprising increasing the temperature of the composition and/or decreasing the total pressure surrounding it and/or by flushing it with a gas stream with no or lower CO<sub>2</sub> content than the gas stream originally applied for the absorption.

### Figures

Figure 1 shows the CO<sub>2</sub> absorption of different ionic liquids comprising selected naturally occurring amino acids.

Figure 2 shows the CO<sub>2</sub> absorption of [N<sub>66614</sub>][Lys] IL at different temperatures.

Figures 3a and 3b show the <sup>1</sup>H-NMR spectra of [N<sub>66614</sub>][Lys] before saturation and after saturation, respectively.

Figure 4 shows three consecutive sorption cycles of [N<sub>66614</sub>][Lys].

Figure 5 shows a reaction scheme showing the proposed mechanism for the proton migration under CO<sub>2</sub> chemisorption on amine group.

Figures 6a-b show selected in situ FTIR spectra of CO<sub>2</sub> absorption (figure 6a) and desorption (figure 6b) of [P66614][Lys] (upper part) and [N66614][Lys] (lower part).

Figure 7 show the full region spectra of (a) [N66614][Lys] under dry CO<sub>2</sub> conditions, (b) [N66614][Lys] under humid CO<sub>2</sub> conditions, (c) [P66614][Lys] under dry CO<sub>2</sub> conditions and (d) [P66614][Lys] under humid CO<sub>2</sub> conditions.

Figure 8 shows a table with a description of the modes highlighted with grey boxes in figure 6a.

Figures 9a-b show the species described in the table in figure 8.

Figure 10 shows quantitative estimates of the carboxylic acid concentration under different humidity concentrations for two ionic liquids as a function of time during CO<sub>2</sub>

exposure. The data is based on the sum of the areas of the deconvoluted spectra of the carboxylic acid C=O stretching bands displayed in figure 7 at around 1700-1695  $\text{cm}^{-1}$ , 1670-1660  $\text{cm}^{-1}$  and 1640-1635  $\text{cm}^{-1}$ .

- 5 Figure 11 shows quantitative estimates of carboxylic acid concentration as a function of time during  $\text{CO}_2$  exposure for (a) [N66614][Lys] under dry  $\text{CO}_2$  conditions, (b) [N66614][Lys] under humid  $\text{CO}_2$  conditions, (c) [P66614][Lys] under dry  $\text{CO}_2$  conditions and (d) [P66614][Lys] under humid  $\text{CO}_2$  conditions.
- 10 Figure 12 shows determination of linear rates from spectral data displayed in figure 7, for (a) [N66614][Lys] under dry  $\text{CO}_2$  conditions, (b) [N66614][Lys] under humid  $\text{CO}_2$  conditions, (c) [P66614][Lys] under dry  $\text{CO}_2$  conditions and (d) [P66614][Lys] under humid  $\text{CO}_2$  conditions .
- 15 Figure 13 shows the very low signal band at around 2335  $\text{cm}^{-1}$  in the in situ FTIR spectra of [N<sub>66614</sub>][Lys] (lower part) and of [P<sub>66614</sub>][Lys] (upper part).

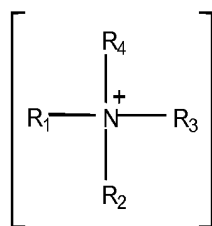
Figure 14 shows TGA data for different functionalized ionic liquids.

## 20 Detailed description of the invention

- The inventors have found that compositions comprising specifically selected ionic liquids (ILs) unexpectedly are excellent absorbers of  $\text{CO}_2$  and are having high sorption efficiencies. Thus, adsorption of super-stoichiometric amounts of  $\text{CO}_2$  at ambient temperature and pressure (i.e. 2 mol  $\text{CO}_2$  per mol IL), are observed. All super-
- 25 stoichiometric uptakes seem to be able to be explainable by chemisorption. The ILs are also excellent absorbers of  $\text{CO}_2$  and are having high sorption efficiencies when adsorbed on high area, porous (including mesoporous) inert materials.

- In a first aspect** the present invention therefore provides a composition for
- 30 absorption/desorption of gaseous carbon dioxide ( $\text{CO}_2$ ). The composition comprises an ionic compound comprising a cation [**A<sup>+</sup>**] and an anion [**B<sup>-</sup>**], wherein wherein the anion [**B<sup>-</sup>**] is a mono-amine functionalized amino acid and the cation [**A<sup>+</sup>**] is given by the formula:





wherein  $R_1$  is a  $C_n$  alkyl chain where  $n$  is an integer having a value of at least 10 and not more than 30, and  $R_2$ ,  $R_3$  and  $R_4$  are individually selected from the group of methyl, ethyl, propyl, butyl, pentyl, hexyl, heptyl and octyl.

Throughout the present application the following abbreviations will be used:

[N66614] = trihexyltetradecylammonium; [N44414] = tributyltetradecylammonium

[N66616] = trihexylhexadecylammonium; [N44416] = tributylhexadecylammonium

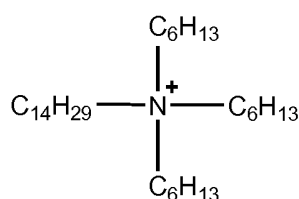
In one or more embodiments  $R_2$ ,  $R_3$  and  $R_4$  are alkyl chains of identical length.

In one or more embodiments  $R_1$  is a  $C_n$  alkyl chain where  $n$  is an integer having a value of between 10 and 20.

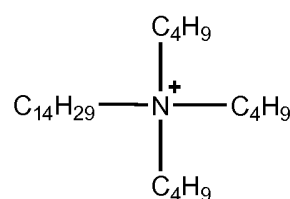
In one or more embodiments  $R_2$ ,  $R_3$  and  $R_4$  are individually selected from butyl, pentyl, hexyl, heptyl and octyl.

In one or more embodiments  $R_1$  is selected from  $C_{14}H_{29}$  and  $C_{16}H_{33}$ , and  $R_2$ ,  $R_3$  and  $R_4$  are individually selected from butyl and hexyl.

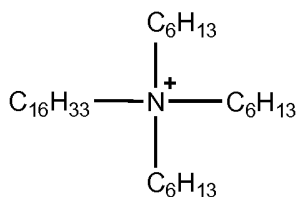
In one or more embodiments the cation is one of the following ammonium ions:



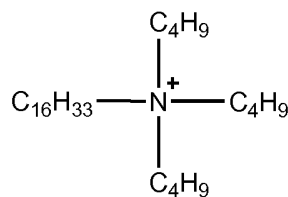
[N66614]



[N44414]



[N66616]



[N44416]

In one or more embodiments the cation is [N66614].

5 In one or more embodiments the cation is [N66616].

In one or more embodiments the cation is [N44414].

In one or more embodiments the cation is [N44416].

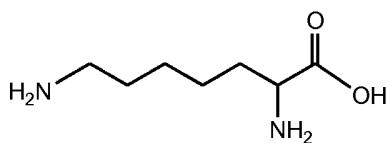
10

In one or more embodiments the anion selected from lysine (Lys), histidine (His), asparagine (Asn), glutamine (Gln). These four amino acids are all having an amine group in addition to the  $\alpha$ -amine group; such amino acids can also be called mono-amine functionalized amino acid.

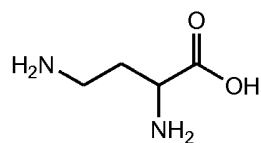
15

In one embodiment the anion selected from proline (Pro) or tryptophan (Trp).

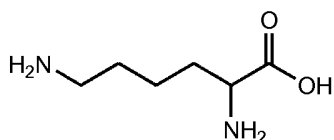
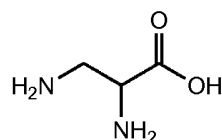
In one or more embodiments, the anion is a mono-amine functionalized amino acid selected from one of the following mono-amine functionalized amino acids:



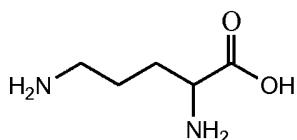
2,7-diaminoheptanoic acid



2,4-diaminobutanoic acid

2,6-diaminohexanoic acid (**Lysine**)

2,3-diaminopropanoic acid

2,5-diaminopentanoic acid (**Ornithine**)

In one or more embodiments the ionic compound is selected from [N44414][Lys], [N44414][Asn], [N44414][Gln] or [N44414][His].

5

In one or more embodiments the ionic compound is selected from [N44416][Lys], [N44416][Asn], [N44416][Gln] or [N44416][His].

In one or more embodiments the ionic compound is selected from [N66614][Lys], [N66614][Asn], [N66614][Gln] or [N66614][His].

10

In one or more embodiments the ionic compound is selected from [N66616][Lys], [N66616][Asn], [N66616][Gln] or [N66616][His].

15

In one or more embodiments the ionic compound is [N66614][Lys].

In one or more embodiments the ionic compound is [N66614][Asn].

In one or more embodiments the ionic compound is [N66614][Gln].

20

In one or more embodiments the ionic compound is [N66614][His].

In one or more embodiments the composition further comprises a high surface area porous inert material such as e.g. a high surface area mesoporous inert material

- 5 In one or more embodiments the high surface area porous inert material is selected from high surface area inorganic, carbonaceous or polymeric materials such as, but not limited to, silica, alumina, titania, zirconia or clays, or mixtures hereof.

- 10 In one or more embodiments, the IL is adsorbed on the high surface area porous inert material, the combined structure referred to as an supported ionic liquid phase (SILP) material.

- 15 In one or more embodiments the porous inert material is selected from **Silica gel 90** (mesh size 80-120, mean pore diameter 74 Å, pore distribution  $\pm 7.0\%$ , pore volume 0.47 cc/g, surface area 152.7 m<sup>2</sup>/g).

- 20 In one or more embodiments the composition according to the **first aspect** of the invention contains between 5-45 % w/w of the ionic compound, such as 10% w/w, 20% w/w, 30% w/w or 40% w/w. Preferably, the ionic compound is selected from [N66614][Lys], [N66614][Asn], [N66614][Gln] or [N66614][His].

- 25 In one or more embodiments the composition according to the **first aspect** of the invention contains about 40% w/w of an ionic compound selected from [N66614][Lys], [N66614][Asn], [N66614][Gln] or [N66614][His].

- 30 In one or more embodiments, the composition of the **first aspect** has a total CO<sub>2</sub> absorption capacity of over about 2 mol CO<sub>2</sub>/mol ionic liquid, such as over 1.8 mol CO<sub>2</sub>/ mol ionic liquid, over 1.9 mol CO<sub>2</sub>/ mol ionic liquid, over 2.0 mol CO<sub>2</sub>/ mol ionic liquid, or over 2.1 mol CO<sub>2</sub>/ mol ionic liquid.

- 35 In one or more embodiments, the composition of the **first aspect** has a total CO<sub>2</sub> absorption capacity of over about 11.0% w/w CO<sub>2</sub>, such as over 11.5% w/w CO<sub>2</sub>, over 11.7% w/w, over 12.0% w/w, over 12.5% w/w, over 12.8% w/w or over 13.1% w/w.

**In a second aspect** the invention provides a method for absorption of gaseous CO<sub>2</sub> from a gas stream, the method comprising contacting said gas stream with a composition according to the **first aspect** of the invention.

5 In one or more embodiments, the invention provides a method according to the **second aspect** of the invention, wherein the absorption takes place from a gas stream which contains 1 – 100 mol% CO<sub>2</sub>, or preferably 2 – 60 mol% CO<sub>2</sub>, or more preferably 3 – 25 mol% CO<sub>2</sub> with an absorption capacity of approximately 2 mol CO<sub>2</sub>/mol of the ionic compound.

10

In one or more embodiments, the contact between the gas stream and the composition takes place in a suitable reactor such as a fixed-bed or movable-bed reactor using an appropriately shaped form of the composition which provides low resistance to the gas stream and low pressure drop across the reactor.

15

In one or more embodiments, the gas stream is a flue-gas stream generated from combustion by large point stationary sources such as power plants.

20

In one or more embodiments, the gas stream contains less than about 15% CO<sub>2</sub> such as 15% CO<sub>2</sub>, 14% CO<sub>2</sub>, 13% CO<sub>2</sub>, 12% CO<sub>2</sub>, 11% CO<sub>2</sub>, 10% CO<sub>2</sub>, 9% CO<sub>2</sub> or between 10-15% CO<sub>2</sub>.

25

In one or more embodiments,, the gas stream contains significant amounts of water vapor, such as 3-5% H<sub>2</sub>O, 5-7% H<sub>2</sub>O, 7-10% H<sub>2</sub>O, 10-12% H<sub>2</sub>O, 12-14% H<sub>2</sub>O 14-16% H<sub>2</sub>O or more than 16% H<sub>2</sub>O.

30

The compositions of the invention may be part of a composite material e.g. combined with fiber materials or other materials which improve the mechanical strength, but do not lower gas diffusion severely.

35

**In a third aspect** the invention also provides a method for desorption of the absorbed CO<sub>2</sub> absorbed on a composition according to the **first aspect** of the invention, the method comprising increasing the temperature of the composition and/or decreasing the total pressure surrounding it and/or by flushing it with a gas stream with no or lower CO<sub>2</sub> content than the gas stream originally applied for the absorption.

When the amine functionalized amino acid ammonium-based ionic liquids (ILs) absorbs CO<sub>2</sub> at a super-equimolar CO<sub>2</sub> absorption capacity of approximately 2 mol of CO<sub>2</sub> per mol of IL at 1 bar pressure it is a 2:1 mechanism.

5

**In a fourth aspect** the invention also provides for the use of a composition according to the above description for the removal of CO<sub>2</sub> in stationary plants such as e.g. power plants, or a flue-gas stream in a power plant.

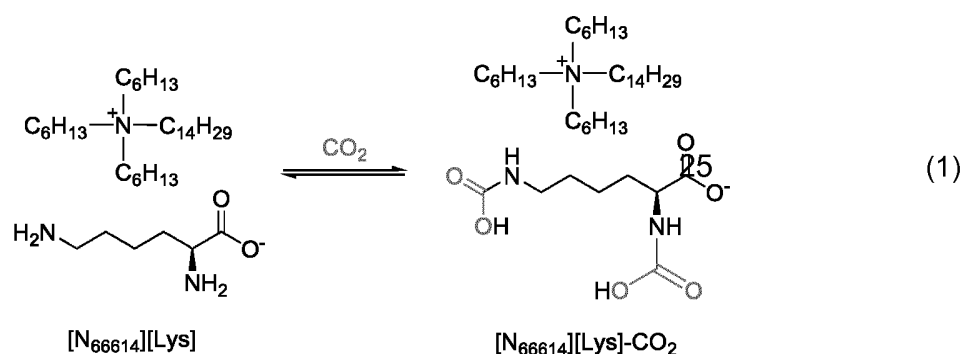
## 10 Experimental

ILs based on the naturally occurring amino acids lysine (Lys), histidine (His), asparagines (Asn), glutamine (Gln), arginine (Arg) and methionine (Met) are employed for the CO<sub>2</sub> absorption study displayed in figure 1 and measured at room temperature (22 °C).

15

The absorption process has been studied with the lysine-based IL trihexyl(tetradecyl)ammonium lysinate ([N<sub>66614</sub>][Lys]) by in situ ATR-FTIR to obtain mechanistic insight on the formation of carbamic acid. The pathway for the formation of the [N<sub>66614</sub>][Lys]-CO<sub>2</sub> adduct is shown in reaction scheme 1 indicating that two CO<sub>2</sub> molecules chemically binds to each a nitrogen in the two amine groups.

20



30

The results are discussed and correlated with mechanistic implications from DFT calculations in the following.

35

Gravimetric CO<sub>2</sub> capacity measurements were initially performed with the series of mono-amine functionalized amino acid ILs; [N<sub>66614</sub>][Lys], [N<sub>66614</sub>][Asn], [N<sub>66614</sub>][Gln] and

- [N<sub>66614</sub>][His] after gas-saturation at ambient conditions. All the ILs showed a remarkable CO<sub>2</sub> absorption capacity equal to  $2.0 \pm 0.1$  mol of CO<sub>2</sub> per mol of IL (3.1-3.5 mol CO<sub>2</sub> per kg of IL, 11.7-13.1 wt.% CO<sub>2</sub>) after 24-48 h gas-saturation at ambient conditions. The results [N<sub>66614</sub>][Asn], [N<sub>66614</sub>][Gln], [N<sub>66614</sub>][His], [N<sub>66614</sub>][Arg] and
- 5 [N<sub>66614</sub>][Met] are shown in figure 1 and the results summarized in table 1, which also includes the results for [N<sub>66614</sub>][Lys] (displayed separately at different temperatures in figure 2) and, for comparison, the lysine-based phosphonium IL [P<sub>66614</sub>][Lys].

<b>Table 1.</b> CO <sub>2</sub> absorption capacity in amine functionalized amino acid ionic liquids				
Ionic liquid	Time (h)	CO <sub>2</sub> uptake		
		Mol CO <sub>2</sub> /mol IL <sup>[*]</sup>	Mol CO <sub>2</sub> /kg IL <sup>[*]</sup>	Wt. %
[N <sub>66614</sub> ][Lys]	24	2.1	3.5	13.1
[N <sub>66614</sub> ][Asn]	24	1.9	3.3	12.0
	48	2.0	3.4	13.1
[N <sub>66614</sub> ][Gln]	24	1.5	2.5	9.5
	48	1.9	3.2	11.7
[N <sub>66614</sub> ][His]	24	1.8	3.0	11.1
	48	1.9	3.1	11.7
[N <sub>66614</sub> ][Arg]	24	1.0	1.6	6.6
	48	1.3	2.1	8.1
[N <sub>66614</sub> ][Met]	4	1.0	1.6	6.9
	24	1.2	1.9	7.8
[P <sub>66614</sub> ][Lys]	-	1.4 <sup>[**]</sup>	2.3 <sup>[**]</sup>	8.7 <sup>[**]</sup>
	48	1.6	2.6	9.9
[*] Relative error estimated to $\pm 0.1$ , [ <sup>**</sup> ] B. F. Goodrich, J. C. de la Fuente, B. E. Gurkan, Z. K. Lopez, E. A. Price, Y. Huang, J. F. Brennecke, <i>J. Phys. Chem.</i> <b>2011</b> , 115, 9140.				

- 10 The results shown in figure 1 and summarized in table 1 suggested that both amine groups in the anions have reacted completely with CO<sub>2</sub> to form [N<sub>66614</sub>][anion]-CO<sub>2</sub> adducts after at the latest 48 hours, as shown in reaction scheme 1 for the IL [N<sub>66614</sub>][Lys].
- 15 Figure 2 shows that during absorption in the [N<sub>66614</sub>][Lys] IL at 22 °C a steep increase of CO<sub>2</sub> absorption is observed which reaches a mol ratio of 1.54 after 3 h, thus implying fast CO<sub>2</sub> absorption dynamics. The slower absorption rate found after 3 h

could in part be due to formation of a hydrogen bonding network making the IL more viscous, thus limiting CO<sub>2</sub> diffusion. However, FT-IR results support a more direct chemical explanation of this decrease in rate, as discussed later.

- 5 In contrast to the homologous series of mono-amine functionalized ILs, the multi-amine [N<sub>66614</sub>][Arg] IL (line with upside down triangles in figure 1) proved to have a significant slower absorption dynamics, and six days were required to reach absorption of two mol CO<sub>2</sub> under identical experimental conditions. Furthermore, the non-functionalized IL [N<sub>66614</sub>][Met] (line with tilted squares in figure 1) absorbed only 1.2 mol  
10 of CO<sub>2</sub> per mol of IL (1.9 mol CO<sub>2</sub> per kg of IL) corresponding to a 1:1 mechanism with an additional amount of gas being physisorbed.

- Brennecke and co-workers [B. F. Goodrich, J. C. de la Fuente, B. E. Gurkan, Z. K. Lopez, E. A. Price, Y. Huang, J. F. Brennecke, *J. Phys. Chem.* **2011**, *115*, 9140.] have  
15 recently reported that the lysine-based phosphonium IL [P<sub>66614</sub>][Lys] absorbed CO<sub>2</sub> corresponding to a mol ratio of 1.4 under ambient conditions. In this study, we found the absorption capacity to be 1.6 mol of CO<sub>2</sub> per mol of IL (2.6 mol CO<sub>2</sub> per kg of IL) in relative good agreement with the earlier results. More importantly, it unambiguously confirming that [N<sub>66614</sub>][Lys] showed a considerable higher CO<sub>2</sub> absorption capacity  
20 than the corresponding [P<sub>66614</sub>][Lys], thus emphasizing the importance of the cation in the system.

- Figure 2 show the influence of the temperature on CO<sub>2</sub> absorption studied for [N<sub>66614</sub>][Lys] between room temperature and 80 °C as a function of time. The initial rate  
25 of absorption increases when the temperature is increased while the absorption capacity decreases, as expected. Hence, after 5 min absorption at 80 °C the CO<sub>2</sub> mol ratio was 0.62, which is 2.3 times higher than at room temperature (see the insert of figure 2).

- 30 After 40 min absorption at 80 °C, the CO<sub>2</sub> absorption capacity reaches a steady-state of about 1 mol CO<sub>2</sub> per mol of IL. Notably, a small mass loss occurs with prolonged treatment at 80 °C under CO<sub>2</sub>-rich conditions, implying that the [N<sub>66614</sub>][Lys]-CO<sub>2</sub> adduct is not thermally stabile at this temperature. Nonetheless, a change in CO<sub>2</sub> absorption capacity by a factor of two induced by a moderate temperature change of  
35 60 °C is very interesting for temperature-swing operated capture processes.



To examine the reactivity of the mono-amine functionalized ILs in more detail, [N<sub>66614</sub>][Lys], [N<sub>66614</sub>][Asn] and [N<sub>66614</sub>][Gln] were analysed by NMR prior to and after saturation with CO<sub>2</sub> for 20 min. Figures 3a and 3b show the results for [N<sub>66614</sub>][Lys] before saturation and after saturation, respectively.

In all the <sup>1</sup>H-NMR (300 MHz, Bruker, DMSO-d<sup>6</sup>) spectra, the signals from the hydrogens on the carbons neighbouring the two amine groups were shifted downfield after interaction with CO<sub>2</sub>. Hence, in the case of [N<sub>66614</sub>][Lys] the signal from the methylene group bonded to the free amine group (H<sub>2</sub>N-CH<sub>2</sub>-) shifted from 2.5 to 2.9 ppm, while the hydrogen on the carbon next to the amino acid group (-OOC-CH-(NH<sub>2</sub>)-) shifted from 2.7 to 3.4 ppm after CO<sub>2</sub> absorption. Similarly, two new carbon signals appeared in <sup>13</sup>C-NMR (50 MHz, Bruker, DMSO-d<sup>6</sup>) for [N<sub>66614</sub>][Lys] after gas-saturation close to each other at 159.6 and 160.1 ppm, respectively, which could be ascribed to the formation of carbamic acid groups. A shift from 176.8 to 175.8 ppm of the signal from the carboxylate carbon further implied that the amine group of the amino acid moiety had reacted with CO<sub>2</sub>. The results supports the hypothesis of [N<sub>66614</sub>][anion]-CO<sub>2</sub> adduct formation as shown in scheme 1.

Following the promising results from the temperature study shown in figure 2a, the reusability of [N<sub>66614</sub>][Lys] in consecutive sorption cycles is next evaluated by performing CO<sub>2</sub> absorption at room temperature and 1 bar CO<sub>2</sub> and desorption at 80 °C under argon flow. The results from three sorption cycles are shown in Figure 4.

During the first desorption process (Des1), 50 % of the absorbed CO<sub>2</sub> (about 1 mol) was liberated after 5 h and 85 % only after 48 h. These results confirmed that the captured CO<sub>2</sub> can be desorbed at elevated temperature under a sweep gas flow, but the process is rather slow especially after the first mol of gas is liberated.

In the second and third sorption cycles (Abs2/Des2 and Abs3/Des3, respectively), the CO<sub>2</sub> absorption capacity remained around the original 2 moles of CO<sub>2</sub> per mol IL after 24 h. Interestingly, it proved here easier to desorb the gas than during the first cycle, thus resulting in initial release of 75 % of the gas (about 1.5 moles of CO<sub>2</sub>), and more than 90 % of the absorbed gas was released after 24 h desorption. The reason behind the difference in desorption efficiency between the first and the following cycles is

currently not clear, but could possibly be related to an initial structural reorganization taking place within the IL during the first sorption cycle.

An overall absorption mechanism for formation of carbamic acids by CO<sub>2</sub>

5 chemisorption in amino acid based ILs has previously been suggested [J. Zhang, S. Zhang, K. Dong, Y. Zhang, Y. Shen, X. Lv. *Chem. Eur. J.* 2006, 12, 4021.] However, the more specific steps in the mechanism have to our knowledge not been discussed in further detail.

10 Here, the transition state energies for two different reaction routes of the first reaction step using DFT (B3LYP/6-31+G\*) is performed, well aware that the energies is likely to be affected by the IL media. However, a solvent model and the cations are not included in the calculations, since solvent property data and diffraction data for the studied IL structures are not available. Without such experimental data inclusion of  
15 cations with specific conformations would most likely not led to an enhancement of the model.

In the first and most simple reaction route, the chemisorption of CO<sub>2</sub> to the amine group is an elemental reaction, where the proton migrates from the amine to an  
20 oxygen atom of the incoming CO<sub>2</sub> molecule. The transition state for this direct one-step proton migration is found to be 139 kJ/mol (relative to the initial physisorption complex). This seems to be a too high value to describe the initial fast reaction rates observed at room temperature for the reaction scheme in figure 5 showing the proposed mechanism for the proton migration under CO<sub>2</sub> chemisorption on amine  
25 group. Calculations were performed with B3LYP/6-31+G(d) Gaussian09.

Therefore an alternative reaction route was investigated, where the proton temporarily forms a five-ring with the carboxylate group of the amino acid group. The transition state for this pathway has a comparable energy of only 21 kJ/mol. Despite the  
30 simplicity of the DFT model, this clearly suggest that the carboxylate group – due to its relative strong basicity – acts like an internal catalyst, which makes the reaction proceed at relatively high rates at room temperature.

To provide further mechanistic insight, the formation of the [N<sub>66614</sub>][Lys]-CO<sub>2</sub> and  
35 [P<sub>66614</sub>][Lys]-CO<sub>2</sub> adducts were also studied by in situ ATR-FTIR. In the setup a thin IL

film was dispersed in the middle of the diamond, and was sealed with a special designed metal cap to allow control of the atmosphere over the film.

In figures 6a-b selected in situ FTIR spectra of the CO<sub>2</sub> absorption (figure 6a) and desorption (figure 6b) experiments are shown, where the upper part is in situ FTIR spectra of [P<sub>66614</sub>][Lys] and the lower part is in situ FTIR spectra of [N<sub>66614</sub>][Lys]. The absorption spectra in figure 6a are measured with the samples exposed to dry CO<sub>2</sub> (60% in He) and the desorption spectra in figure 6b are measured under helium flow at 80°C.

Figure 7, part (a) shows [N<sub>66614</sub>][Lys] under dry CO<sub>2</sub> conditions, part (b) [N<sub>66614</sub>][Lys] under humid CO<sub>2</sub> conditions, part (c) [P<sub>66614</sub>][Lys] under dry CO<sub>2</sub> conditions, and part (d) [P<sub>66614</sub>][Lys] under humid CO<sub>2</sub> conditions. The dark lines in both figures 6a-b and figure 7 correspond to initial times, lighter lines to later times and dashed lines to (pseudo) steady-state in the experiments.

Figure 8 displays a table with a description of the modes highlighted with grey boxes in figure 6a, and figures 9a-b show the species described in the table in figure 8.

The initial spectrum of the [N<sub>66614</sub>][Lys] IL displayed in figure 6a reveals characteristic vibration modes of the **carboxylate group** ( $\nu_{\text{O-C-O,asym}} = 1588 \text{ cm}^{-1}$ ) and primary amines ( $\nu_{\text{N-H}} = 3360 \text{ and } 3280 \text{ cm}^{-1}$ ,  $\delta_{\text{N-H}} = 1660 \text{ and } 844 \text{ cm}^{-1}$ ). Upon CO<sub>2</sub> exposure the modes of the primary amines in the IL disappeared. Simultaneously characteristic modes of a **carboxylic acid dimer** ( $\nu_{\text{O-C-O,asym}} = 1697 \text{ cm}^{-1}$ ) together with carboxylic acid species **hydrogen bonded to the carboxylate group** ( $\nu_{\text{O-C-O,asym}} = 1660\text{-}1645 \text{ cm}^{-1}$ ) appeared, as also reported previously.<sup>[10]</sup> After a few minutes of gas exposure the rate of reaction apparently decreased drastically (as the reaction approached steady-state), and the band corresponding to the carboxylate group ( $\nu_{\text{O-C-O,asym}}$ ) blue shifted around  $15 \text{ cm}^{-1}$  indicating changes in the hydrogen bonding to the carboxylate group.

The series of spectra shown in figure 6b show the reversible desorption of CO<sub>2</sub> from the [N<sub>66614</sub>][Lys] IL (lower part) and [P<sub>66614</sub>][Lys] IL (upper part), which are analogous to the results of the absorption experiments shown in figure 2.

As the in situ FT-IR experiments are performed on a very thin IL film, the reaction time to approach steady-state is much shorter than for the bulk absorption experiments due to faster diffusion in the film layer. To get an estimate of the reaction kinetics for the IL-CO<sub>2</sub> adduct formation, the amount of carboxylic acids is quantified as function of time for selected ILs by integrating the deconvoluted bands of the  $\nu_{\text{O-C-O,asym}}$  of the carboxylic acid species. The results are shown in figure 10, which shows quantitative estimates of the carboxylic acid concentration as a function of time during CO<sub>2</sub> exposure (60 % in He). The estimate is based on the sum of the areas of the carboxylic acid C=O stretching bands at around 1700-1695 cm<sup>-1</sup>, 1670-1660 cm<sup>-1</sup> and 1640-1635 cm<sup>-1</sup> of the deconvoluted spectra.

The details on each of these bands are shown in figure 11 and 12, where figure 11 shows quantitative estimates of carboxylic acid concentration as a function of time during CO<sub>2</sub> exposure. Estimate is based on the areas of the carboxylic acid C=O stretching bands at around 1700-1695 cm<sup>-1</sup>, 1670-1660 cm<sup>-1</sup> and 1640-1635 cm<sup>-1</sup> of the deconvoluted spectra. Absolute scale on y axis is established from spectra of [N<sub>66614</sub>][Lys] exposed to CO<sub>2</sub> for 19 h assuming 2 mole of carboxylic acid per mol IL. Figure 12 shows determination of linear rates (mol s<sup>-1</sup>) from spectral data corresponding to figure 7.

In both figure 11 and 12, part (a) shows [N<sub>66614</sub>][Lys] under dry CO<sub>2</sub> conditions, part (b) [N<sub>66614</sub>][Lys] under humid CO<sub>2</sub> conditions, part (c) [P<sub>66614</sub>][Lys] under dry CO<sub>2</sub> conditions, and part (d) [P<sub>66614</sub>][Lys] under humid CO<sub>2</sub> conditions.

Initially, a non-linear diffusion controlled domain is observed for [N<sub>66614</sub>][Lys]. This domain is influenced by the viscosity of the IL as well as the specific thickness of the IL film on the ATR plate varying from experiment to experiment. At the same time almost no physisorbed CO<sub>2</sub> was observed in the spectra of [N<sub>66614</sub>][Lys] as it instantly reacts with the amine groups. This can be seen from the details in figure 13 showing the very low signal band at around 2335 cm<sup>-1</sup> in the in situ FTIR spectra of [N<sub>66614</sub>][Lys] (lower part) and of [P<sub>66614</sub>][Lys] (upper part).

After around 10-12 min of absorption the estimated development in carboxylic acid concentration approaches a linear rate corresponding to pseudo zero-order (see table 2). This interpretation is strongly supported by development in the physisorbed CO<sub>2</sub>,

which shows that the main CO<sub>2</sub> diffusion layer at this time reached the evanescent beam in the bottom of the film (see absorbance of physisorbed CO<sub>2</sub> at around 2335 cm<sup>-1</sup> in figure 13). Here, the kinetics is no longer controlled by diffusion limitations but by a reaction barrier for the reaction between CO<sub>2</sub> and the amine groups. This results in a linear development of the carboxylic acid product (i.e. pseudo zero-order reaction kinetics) and a slow net accumulation of physisorbed CO<sub>2</sub>.

Table 2

Experiment	Apparent rate (mol·s <sup>-1</sup> )	R <sup>2</sup>	Steady-state yield
[N <sub>66614</sub> ][Lys] (dry)	2.1·10 <sup>-4</sup>	0.9940	2.00 mol (19 h) <sup>a</sup>
[N <sub>66614</sub> ][Lys] (1.1% water)	2.6·10 <sup>-4</sup>	0.9960	1.47 mol (4 h)
[N <sub>66614</sub> ][Lys] (0.22% water)	2.1·10 <sup>-4</sup>	0.9950	1.43 (26 min) <sup>b</sup>
[P <sub>66614</sub> ][Lys] (dry)	9.2·10 <sup>-4</sup>	0.9968	1.10 (2 h)
[P <sub>66614</sub> ][Lys] (2.0% water)	56·10 <sup>-4</sup>	0.9972	0.72 (2 h)

<sup>a</sup> This is assumed to be real steady-state and 2.00 mol from the adsorption experiments. <sup>b</sup> The number corresponds to a pseudo steady-state as the experiments were stopped before a real steady-state occurred.

- 10 As the reaction approached full conversion (i.e. complete reaction of CO<sub>2</sub> with the amine groups), the rate decreases and physisorbed CO<sub>2</sub> quickly accumulates in the IL resulting in a sudden shift of the carboxylate  $\nu_{O-C-O, asym}$ . As mentioned above, this may partly be explained by an increased viscosity of the system. Notably, however, the reaction rate decreases dramatically after 1.7-1.8 mol carboxylic acid per mol
- 15 [N<sub>66614</sub>][Lys] had reacted, despite physisorbed CO<sub>2</sub> at this time is in surplus.

Considering the suggested mechanism, a likely explanation for this behaviour is that the carboxylic acid in the lysinate at this stage is so strongly hydrogen bonded to the carboxylate group that it no longer acts efficiently as a catalyst for the chemisorption of

20 CO<sub>2</sub>. It is also noticeable that no break on the absorption curve occurs before the 1.7-1.8 mol CO<sub>2</sub> per mol [N<sub>66614</sub>][Lys] is absorbed (see figure 2), thus suggesting equal

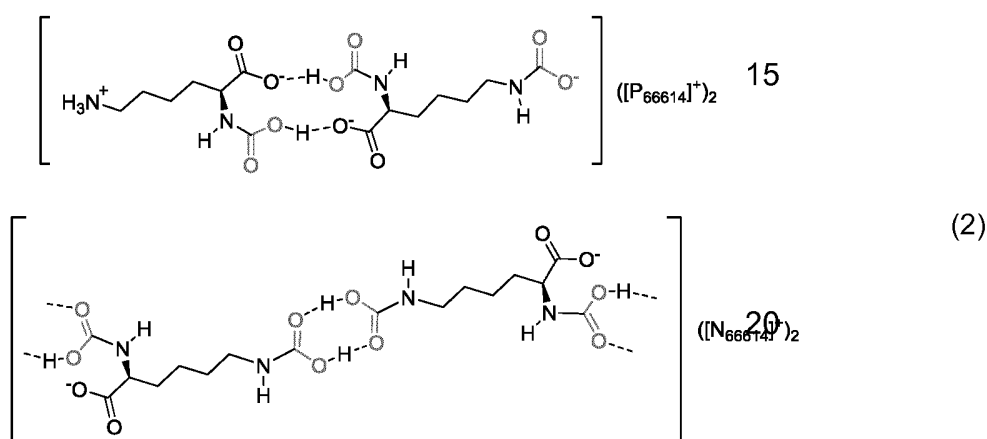
reaction rates – and possibly similar mechanism for CO<sub>2</sub> absorption – at the two amine groups.

Several studies report that addition of water to ILs enhances the apparent CO<sub>2</sub> absorption rate due to a decrease in viscosity. For the [N<sub>66614</sub>][Lys] IL an increase of the first order chemisorption rate of about 20 % from  $2.1 \cdot 10^{-4}$  to  $2.6 \cdot 10^{-4}$  mol/s (see table 2) was observed, when the IL was saturated with a water concentration corresponding to 1.1 vol% in the gas stream. With lower water concentrations this rate enhancement is not observed, suggesting that water may stabilize a transition state in the critical proton migrating step in the mechanism – possibly by a push-pull type mechanism – facilitating the proton transfer. Accordingly, the steady-state CO<sub>2</sub> absorption capacity is also lowered in presence of water compared to the water free system, due to competitive hydrogen bonding of the water to the carboxylic acid-carboxylate pair as can be seen in figure 10.

As no significant cationic effect was made obvious from the theoretical studies, in-situ ATR-FTIR investigations is also performed on the [P<sub>66614</sub>][Lys] during CO<sub>2</sub> absorption and the results displayed in the top part of figure 6a. Here the dominant band for the carboxylic acid species formed during CO<sub>2</sub> absorption is not the dimeric 1700 cm<sup>-1</sup> band, as found for the [N<sub>66614</sub>][Lys] IL. Instead the band appearing at around 1640 cm<sup>-1</sup> is far more intense, thus indicating that the formed carboxylic acid groups preferentially pairs up with the carboxylate groups instead of forming dimers.

This interpretation is further confirmed by the observation of a fast shift in intensity of the carboxylate band at around 1590 cm<sup>-1</sup> simultaneously with the rise of the 1640 cm<sup>-1</sup> band, indicating a much stronger hydrogen bonding between carboxylic acid and carboxylate groups than seen during CO<sub>2</sub> absorption in [N<sub>66614</sub>][Lys]. Furthermore, the pseudo zero-order rate of CO<sub>2</sub> chemisorption is more than four times higher with [P<sub>66614</sub>][Lys] than for [N<sub>66614</sub>][Lys] ( $9.2 \cdot 10^{-4}$  mol/s vs.  $2.1 \cdot 10^{-4}$  mol/s, as listed in table 2) until absorption reached about 0.9 mol CO<sub>2</sub> per mol IL. After this point – where the carboxylate groups are almost stoichiometric hydrogen bonded to the formed carboxylic acid and thus not catalytically effective for chemisorption – the rate decreases significantly with around three orders of magnitude. Afterwards chemisorption continues only slowly up to 1.5 mol CO<sub>2</sub> per mol IL, most likely by a very different mechanism having a much higher reaction barrier.

Another obvious difference in the spectra recorded during CO<sub>2</sub> absorption with [P<sub>66614</sub>][Lys] and [N<sub>66614</sub>][Lys] as shown in figure 6a is the appearance of a strong N-H stretching band at around 3400 cm<sup>-1</sup> for the phosphonium IL (see inserts on in figure 6a). The high position of the band suggests that nitrogen is linked to a very electronegative group. This observation together with the striking break in the absorption rate around 0.9-1 mol absorbed CO<sub>2</sub> and the apparent maximum absorption capacity of 1.5 mol CO<sub>2</sub> per mol [P<sub>66614</sub>][Lys] make us suggest, that half a mol of CO<sub>2</sub> is absorbed in this IL (under dry conditions) as a carbamate creating a NH<sub>3</sub><sup>+</sup> group and a COO<sup>-</sup> group. Hence, we propose that the [P<sub>66614</sub>][Lys]-CO<sub>2</sub> and [N<sub>66614</sub>][Lys]-CO<sub>2</sub> adducts comprise two different anion structures, as schematically shown in reaction scheme (2) below.



The apparent viscosity of the neat [N<sub>66614</sub>][Lys] IL is significantly higher (> 200 mPa/s at 80 °C) than for the [P<sub>66614</sub>][Lys] IL. This suggests weaker interactions between the carboxylate of the lysinate anion and the cations in the latter liquid, thus initially making the catalytically active carboxylate group more accessible in [P<sub>66614</sub>][Lys] than in [N<sub>66614</sub>][Lys] during CO<sub>2</sub> absorption. Accordingly, the chemisorption kinetics is faster in the phosphonium IL, but the capacity is lower due to competitive formation of strongly hydrogen bonded complexes with the formed carboxylic acids.

Figure 14 shows the thermal stability of the different functionalized ionic liquids N<sub>66614</sub>[Lys], [N<sub>66614</sub>][Asn], [N<sub>66614</sub>][Gln], [N<sub>66614</sub>][His], [N<sub>66614</sub>][Arg], and [N<sub>66614</sub>][Met] according to this invention measured by TGA analysis.

The temperature stability of the ILs can be estimated from the TGA results, where the point of decomposition is determined by initial curvature of both the curve representing the weight as well as the heat flux to the sample. The points of decomposition for all the pure ILs were measured to be 140–150 °C.

5

The above described figures individually and/or in combination show that amine functionalized amino acid ILs like, e.g. [N<sub>66614</sub>][Lys] absorb CO<sub>2</sub> gas at ambient conditions corresponding to unprecedented  $2.0 \pm 0.1$  mol of CO<sub>2</sub> per mol of IL (3.5 mol CO<sub>2</sub> per kg IL, 13.1 wt.% CO<sub>2</sub>).

10

At elevated temperature of 80 °C, the absorption capacity of [N<sub>66614</sub>][Lys] is equal to 1 mol CO<sub>2</sub> per mol of IL, demonstrating that it is possible to desorb the CO<sub>2</sub> gas under CO<sub>2</sub>-rich conditions by temperature-swing absorption. Moreover, the recycling experiments of figure 4 confirms the successful use of the IL in three consecutive sorption cycles, apparently even with an improved performance after the first cycle.

15

Mechanistic investigations of the absorption process by NMR and in situ FTIR studies reveals, that CO<sub>2</sub> absorption in the [N<sub>66614</sub>][Lys] IL results in formation of carbamic acids by reaction of CO<sub>2</sub> with the amine groups according to a 2:1 mechanism, where the amino acid carboxylate group plays an important catalytic role for fast absorption up to 1.8 moles of CO<sub>2</sub>. This seems to be due to the carboxylic acids formed arrange as acid-acid dimers with only little interaction with the carboxylate group, thus allowing the reaction to proceed until almost stoichiometric conversion.

20

For the analogous phosphonium-based IL, [P<sub>66614</sub>][Lys], a very fast initial CO<sub>2</sub> absorption rate up to 0.9 moles of CO<sub>2</sub> is observed, where after the rate decreased dramatically as the formed acid species hydrogen bonded strongly with the carboxylate group thereby inhibiting its catalytic effect. The origin of the cationic effect is speculated to be correlated to the strength of the ion interactions in the two different ILs.

30

#### *Experimental details*

##### *NMR studies*



$^1\text{H}$  (300 MHz) and  $^{13}\text{C}$ -NMR (75 and 50MHz) spectra were recorded on a Bruker AM360 NMR spectrometer in  $\text{D}_2\text{O}$ ,  $\text{CD}_3\text{CN}$ ,  $\text{CD}_4\text{OD}$  or  $\text{DMSO-d}_6$  at 25 °C. The NMR results obtained (and shown in figures 3a-b for  $[\text{N}_{66614}][\text{Lys}]$ ) are the following:

5  *$[\text{N}_{66614}][\text{Lys}]$  prior to saturation*

$^1\text{H}$ -NMR (300 MHz,  $\text{D}_2\text{O}$ ):  $\delta/\text{ppm}$  = 0.7-0.8 (m, 12H; 4 $\text{CH}_3$ ), 1.05-1.7 (m, 54H; 27 $\text{CH}_2$ ), 2.4 (t, 2H;  $\text{CH}_2$ ), 2.9-3.2 (m, 9H; 4 $\text{CH}_2$  & CH);  $^{13}\text{C}$ -NMR (75.5 MHz,  $\text{CD}_3\text{OD}$ ):  $\delta/\text{ppm}$  = 13.4, 13.6, 21.6, 22.5, 22.7, 22.8, 26.0, 29.4, 29.6, 29.7, 29.8, 31.3, 32.0, 33.1, 35.7, 41.5, 47.4, 47.6, 47.9, 48.2, 48.5, 48.9, 56.8, 58.7, 181.3.  $^1\text{H}$ -NMR (300 MHz,  $\text{DMSO-d}_6$ ):  $\delta/\text{ppm}$  = 0.8-1.0 (m, 12H; 4 $\text{CH}_3$ ), 1.1-1.4 (m, 44H; 22 $\text{CH}_2$ ), 1.4-1.65 (m, 10H; 5 $\text{CH}_2$ ), 2.5 (m, 2H;  $\text{CH}_2$ ), 2.7 (t, 1H;  $\text{CH}_2$ ), 3.1-3.3 (m, 8H; 4 $\text{CH}_2$ );  $^{13}\text{C}$ -NMR (50 MHz,  $\text{DMSO-d}_6$ ):  $\delta/\text{ppm}$  = 13.7, 13.8, 21.0, 21.9, 22.1, 23.6, 25.4, 25.7, 28.3, 28.7, 29.0, 30.6, 31.3, 34.0, 34.5, 36.4, 41.9, 56.4, 57.6, 176.8.

15  *$[\text{N}_{66614}][\text{Lys}]$  after  $\text{CO}_2$  saturation*

$^1\text{H}$ -NMR (300 MHz,  $\text{DMSO-d}_6$ ):  $\delta/\text{ppm}$  = 0.8-1.0 (m, 12H; 4 $\text{CH}_3$ ), 1.1-1.4 (m, 44H; 22 $\text{CH}_2$ ), 1.4-1.65 (m, 10H; 5 $\text{CH}_2$ ), 2.9 (m, 2H;  $\text{CH}_2$ ), 3.4 (t, 1H;  $\text{CH}_2$ ), 3.1-3.3 (m, 8H; 4 $\text{CH}_2$ );  $^{13}\text{C}$ -NMR (50 MHz,  $\text{DMSO-d}_6$ ):  $\delta/\text{ppm}$  = 13.5, 21.0, 21.8, 22.0, 22.9, 25.4, 25.6, 26.5, 26.8, 28.3, 28.7, 29.0, 30.2, 30.5, 31.3, 32.6, 34.0, 53.5, 55.6, 57.6, 60.4, 159.6, 160.1, 175.8.

*$[\text{N}_{66614}][\text{Asn}]$  prior to  $\text{CO}_2$  saturation*

$^1\text{H}$ -NMR (300 MHz,  $\text{CD}_3\text{CN}$ ):  $\delta/\text{ppm}$  = 1.4-1.5 (m, 12H; 4 $\text{CH}_3$ ), 1.8-2.0 (m, 40H; 20 $\text{CH}_2$ ), 2.1-2.25 (m, 8H; 4 $\text{CH}_2$ ), 2.65-3.1 (m, 2H; 1 $\text{CH}_2$ ), 3.6-3.7 (m, 8H; 4 $\text{CH}_2$ ), 3.7-3.8 (t, 1H, CH);  $^1\text{H}$ -NMR (300 MHz,  $\text{DMSO-d}_6$ ):  $\delta/\text{ppm}$  = 0.8-1.0 (m, 12H; 4 $\text{CH}_3$ ), 1.2-1.4 (m, 40H; 20 $\text{CH}_2$ ), 1.4-1.65 (m, 8H; 4 $\text{CH}_2$ ), 1.9-2.42 (m, 2H; 1 $\text{CH}_2$ ), 3.1 (t, 1H, CH), 3.1-3.25 (m, 8H; 4 $\text{CH}_2$ );  $^{13}\text{C}$ -NMR (75.5 MHz,  $\text{CD}_3\text{CN}$ ):  $\delta/\text{ppm}$  = 13.3, 14.0, 21.8, 22.6, 22.9, 26.1, 26.3, 29.1, 29.5, 29.6, 29.7, 29.86, 29.9, 30.0, 31.4, 32.1, 43.5, 49.5, 54.5, 58.7, 175.8, 177.4.

*$[\text{N}_{66614}][\text{Asn}]$  after  $\text{CO}_2$  saturation*

$^1\text{H}$ -NMR (300 MHz,  $\text{DMSO-d}_6$ ):  $\delta/\text{ppm}$  = 0.8-1.0 (m, 12H; 4 $\text{CH}_3$ ), 1.2-1.4 (m, 40H; 20 $\text{CH}_2$ ), 1.4-1.65 (m, 8H; 4 $\text{CH}_2$ ), 2.2-2.5 (m, 2H; 1 $\text{CH}_2$ ), 3.1-3.25 (m, 8H; 4 $\text{CH}_2$ ), 3.75 (t, 1H, CH).

*[N<sub>66614</sub>][Gln] prior to CO<sub>2</sub> saturation*

<sup>1</sup>H-NMR (300 MHz, DMSO-d<sub>6</sub>): δ/ppm = 0.8-0.1 (m, 12H; 4CH<sub>3</sub>), 1.2-1.4 (m, 40H; 20CH<sub>2</sub>), 1.4-2.2. (m, 12H; 6CH<sub>2</sub>), 2.8 (t, 1H, CH), 3.1-3.3 (m, 8H, 4CH<sub>2</sub>); <sup>13</sup>C-NMR (75.5 MHz, DMSO-d<sub>6</sub>): δ/ppm = 14.4, 14.5, 21.8, 22.7, 22.9, 26.2, 29.1, 29.2, 29.5, 29.7,  
5 29.9, 31.4, 32.1, 33.5, 33.9, 49.9, 56.6, 58.3, 176.2, 177.4.

*[N<sub>66614</sub>][Gln] after CO<sub>2</sub> saturation*

<sup>1</sup>H-NMR (300 MHz, DMSO-d<sub>6</sub>): δ/ppm = 0.8-0.1 (m, 12H; 4CH<sub>3</sub>), 1.2-1.4 (m, 40H; 20CH<sub>2</sub>), 1.4-1.6 (m, 8H; 4CH<sub>2</sub>), 1.6-2.1 (m, 4H; 2CH<sub>2</sub>), 3.1-3.3 (m, 8H, 4CH<sub>2</sub>), 3.4 (t,  
10 1H, CH).

*[N<sub>66614</sub>][His] after CO<sub>2</sub> saturation*

<sup>1</sup>H-NMR (300 MHz, DMSO-d<sub>6</sub>): δ/ppm = 0.8-0.1 (m, 12H; 4CH<sub>3</sub>), 1.2-1.4 (m, 40H; 20CH<sub>2</sub>), 1.4-1.7 (m, 8H; 4CH<sub>2</sub>), 2.85-3.0 (m, 2H, 1 CH<sub>2</sub>), 3.1 (t, 1H, CH), 3.1-3.3 (m,  
15 8H, 4CH<sub>2</sub>), 6.6 (s, 1H, Ar-CH), 7.4 (s, 1H, Ar-CH).

*[N<sub>66614</sub>][Arg] after CO<sub>2</sub> saturation*

<sup>1</sup>H-NMR (300 MHz, DMSO-d<sub>6</sub>): δ/ppm = 0.8-0.1 (m, 12H; 4CH<sub>3</sub>), 1.0-1.3 (m, 42H; 21CH<sub>2</sub>), 1.4-1.6 (m, 8H; 4CH<sub>2</sub>), 2.15 (m, 2H, 1 CH<sub>2</sub>), 2.85 (t, 1H, CH), 2.95 (m, CH,  
20 1CH<sub>2</sub>), 3.0-3.2 (m, 8H, 4CH<sub>2</sub>).

*[N<sub>66614</sub>][Met] after CO<sub>2</sub> saturation*

<sup>1</sup>H-NMR (300 MHz, D<sub>2</sub>O): δ/ppm = 0.7-0.8 (m, 12H; 4CH<sub>3</sub>), 1.05-1.3 (m, 40H; 20CH<sub>2</sub>), 1.4-1.6 (m, 8H, 4CH<sub>2</sub>), 1.6-1.9 (m, 2H, CH<sub>2</sub>) 1.95 (s, 3H, CH<sub>3</sub>), 2.4 (t, 2H; CH<sub>2</sub>), 3.0-  
25 3.1 (m, 8H; 4CH<sub>2</sub>), 3.2 (t, 1H, CH); <sup>13</sup>C-NMR (75.5 MHz, CD<sub>3</sub>OD): δ/ppm = 13.3, 13.4, 13.6, 21.6, 22.4, 22.7, 25.9, 26.0, 29.2, 29.4, 29.7, 29.73, 30.5, 31.2, 32.0, 35.7, 56.1, 58.2, 181.0.

*Synthesis of [P<sub>66614</sub>][Lys]*

30 15 mmol of trihexyl(tetradecyl)phosphonium bromide ([P<sub>66614</sub>][Br]) was dissolved in 10 ml of methanol and 1.2 equivalent of amberlite IRA 400 (OH) ion exchange resin added to the mixture. The reaction mixture was allowed to stir to ion-exchange at room temperature. After 24h, resin was filtered off and 1.2 equivalent fresh amberlite IRA 400 (OH) resin added to the filtrate. The same procedure was repeated three times to  
35 get the maximum ion-exchanged [P<sub>66614</sub>][OH] ionic liquid in methanol. After the third

ion-exchange, methanolic solution of  $[P_{66614}][OH]$  was neutralised with slightly excess equimolar amount of lysine and allowed to stir overnight. The methanol was evaporated and the unreacted amino acid was removed by using cold acetonitrile to get the ionic liquid  $[P_{66614}][Lys]$ . The unexchanged bromide was measured in Metrohm ion chromatography and it was found to be 3200 ppm. The bromide content was quantified from series of standards of  $[P_{66614}][Br]$ .

$^1H$ -NMR (300 MHz,  $D_2O$ )  $\delta$  = 0.7-0.8 (m, 12H; 4CH<sub>3</sub>), 1.05-1.65 (m, 54H; 27CH<sub>2</sub>), 2.5 (t, 2H; CH<sub>2</sub>), 2.95-3.2 (m, 9H; 4CH<sub>2</sub> and CH) ;  $^1H$ -NMR (300 MHz, DMSO- $d_6$ ):  $\delta/ppm$  = 0.8-1.0 (m, 12H; 4CH<sub>3</sub>), 1.2-1.6 (m, 54H; 27CH<sub>2</sub>), 2.1-2.3 (m, 8H; 4CH<sub>2</sub>), 2.5 (m, 2H; CH<sub>2</sub>), 2.65 (t, 1H; CH<sub>2</sub>);  $^{13}C$ -NMR (75.5 MHz, MeOH- $d_4$ )  $\delta$  = 13.40, 13.47, 13.59, 13.63, 21.57, 21.63, 22.46, 22.72, 23.23, 25.96, 26.20, 29.03, 29.41, 29.44, 29.50, 29.58, 29.64, 29.73, 29.75, 29.77, 31.28, 31.94, 32.03, 33.10, 35.53, 41.47, 56.52, 58.22, 58.37, 181.14.;  $^{13}C$ -NMR (50 MHz, DMSO- $d_6$ ):  $\delta/ppm$  = 14.4, 14.5, 18.0, 18.6, 21.4, 21.5, 22.6, 22.8, 24.4, 29.0, 29.5, 29.8, 30.5, 30.7, 31.2, 32.1, 34.7, 42.7, 49.5, 57.1, 177.6.

#### *TGA analysis, general procedure*

Thermo gravimetric analysis (TGA) was performed on a Mettler Toledo TGA/DSC 1 STAR System with a Gas Controller GC 100 and a flow of nitrogen of 70 mL/min. A crucible was weighed inside the TGA instrument and approximately 5-15 mg of IL was transferred to it before reinsertion. The weight was noted and during measurements samples were heated from 40 to 600 °C at a constant heating rate of 10 °C/min under nitrogen atmosphere.

#### *CO<sub>2</sub> sorption studies*

CO<sub>2</sub> absorptions were carried out with 1-2 g of neat amino acid ILs in a closed vessel by bubbling CO<sub>2</sub> (99.990 %, Air Liquide) through the liquid at various temperatures at atmospheric pressure. Desorption was performed at 80 °C under an argon flow. The CO<sub>2</sub> absorption capacity was measured with a gravimetric balance (0.1 mg accuracy) by weighing the vessel periodically during the sorption experiments.

#### *In situ ATR-FTIR studies*

IR spectra of the amino acid ILs were recorded on a Nicolet iS5 spectrometer (8 scans, 4 cm<sup>-1</sup> resolution) equipped with a heatable diamond ATR cell (GladiATR, Pike

Technologies) and a special gas absorption add-on device. The IL samples were outgassed in situ at 80 °C in 100 mL/min He before being exposed to a gas mixture of 60:40 vol% CO<sub>2</sub>:He at a flow of 35 mL/min. Helium was either used dry or humidified with water vapour. Desorption experiments were performed at 80 °C. All spectra were

5 ATR corrected using OMNIC software assuming a refractive index of 1.5. A special deconvolution procedure was developed to accurately determine the area of the carboxylate bands at 1700-1695, 1670-1660 and 1640-1635 cm<sup>-1</sup>. Initially we aimed to determine the band areas related to the carboxylic acids species from the difference spectra (IL+CO<sub>2</sub> spectra at a given time minus the spectra of the outgassed IL).

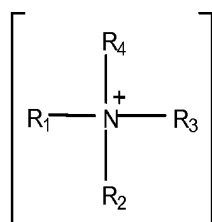
10 However, this proved unpractical as the neighbouring C=O stretching bands from the carboxylate group at around 1590 cm<sup>-1</sup> shifted significantly during the CO<sub>2</sub> absorption. The problem was solved by first fitting a spectrum of the pure outgassed IL -before CO<sub>2</sub> absorption - with nine Gaussian functions where the sum of the functions served as background spectra. Then the Gaussian function equivalent to the carboxylate C=O

15 stretching band was removed from the static background sum-function and the quasi-difference spectrum deconvoluted. The spectrum at a given time during CO<sub>2</sub> exposure minus the manipulated background function was then fitted, thereby allowing the bands of the carboxylate group to act dynamic and thus enhance the accuracy of the deconvolution. A script package was developed using Gnuplot 4 to automate the

20 deconvolution of the large amounts of spectra needed to establish the presented kinetic data.

**CLAIMS**

1. A composition for absorption/desorption of gaseous carbon dioxide (CO<sub>2</sub>), the composition comprising an ionic compound comprising a cation **[A<sup>+</sup>]** and an anion **[B<sup>-</sup>]**, wherein the anion **[B<sup>-</sup>]** is a mono-amine functionalized amino acid and the cation **[A<sup>+</sup>]** is given by the formula:



wherein R<sub>1</sub> is a C<sub>n</sub> alkyl chain where n is an integer having a value of at least 10 and not more than 30, and R<sub>2</sub>, R<sub>3</sub> and R<sub>4</sub> are individually selected from the group of methyl, ethyl, propyl, butyl, pentyl, hexyl, heptyl and octyl.

10

2. A composition according to claim 1, wherein R<sub>2</sub>, R<sub>3</sub> and R<sub>4</sub> are individually selected from the group of ethyl, propyl, butyl, pentyl, hexyl, heptyl and octyl.

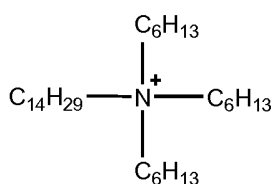
15

3. A composition according to claim 1 or 2, wherein R<sub>2</sub>, R<sub>3</sub> and R<sub>4</sub> are alkyl chains of identical length.

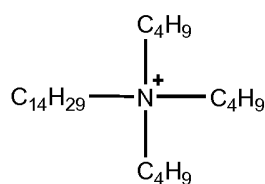
4. A composition according to any preceding claim, wherein R<sub>1</sub> is selected from C<sub>14</sub>H<sub>29</sub> and C<sub>16</sub>H<sub>33</sub>, and R<sub>2</sub>, R<sub>3</sub> and R<sub>4</sub> are individually selected from butyl and hexyl.

20

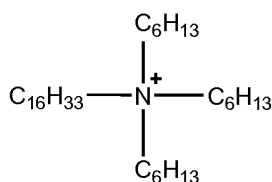
5. A composition according to any preceding claim, wherein the cation is one of the following ammonium ions:



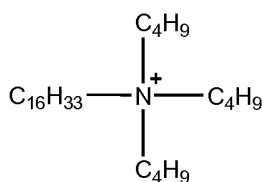
[N66614]



[N44414]



[N66616]



[N44416]

6. A composition according to claim 5, wherein the cation is [N66614].

5 7. A composition according to claim 5, wherein the cation is [N66616].

8. A composition according to claim 5, wherein the cation is [N44414].

9. A composition according to claim 5, wherein the cation is [N44416].

10

10. A composition according to any preceding claim, wherein the anion is selected from lysine (Lys), histidine (His), asparagine (Asn), glutamine (Gln).

11. A composition according to claim 10, wherein the ionic compound is selected from [N66614][Lys], [N66614][Asn], [N66614][Gln] or [N66614][His].

15

12. A composition according to any preceding claim, wherein the composition further comprises a high surface area porous inert material such as e.g. a high surface area mesoporous inert material.

20

13. A composition according to claim 12, wherein the high surface area porous inert material is selected from high surface area inorganic, carbonaceous or polymeric materials such as, but not limited to, silica, alumina, titania, zirconia or clays, or mixtures hereof.

25

14. A composition according to claim 12 or 13, wherein the ionic compound is adsorbed on the high surface area porous inert material, the combined structure referred to as a supported ionic liquid phase (SILP) material.
- 5 15. A method for absorption of gaseous CO<sub>2</sub> from a gas stream, the method comprising contacting said gas stream with a composition according to any preceding claims.
- 10 16. A method for absorption of gaseous CO<sub>2</sub> from a gas stream according to claim 15, wherein the gas stream contains 1 – 100 mol% CO<sub>2</sub>, or preferably 2 – 60 mol% CO<sub>2</sub>, or more preferably 3 – 25 mol% CO<sub>2</sub> with an absorption capacity of approximately 2 mol CO<sub>2</sub>/mol of the ionic compound.
- 15 17. A method for absorption of gaseous CO<sub>2</sub> from a gas stream according to claim 15 or 16 wherein the contact between the gas stream and the composition takes place in a suitable reactor such as a fixed-bed or movable-bed reactor using an appropriately shaped form of the composition adapted for providing low resistance to the gas stream and low pressure drop across the reactor.
- 20 18. A method for desorption of CO<sub>2</sub> absorbed on a composition according to any of claims 1-14, the method comprising increasing the temperature of the composition and/or decreasing the total pressure surrounding it and/or by flushing it with a gas stream with no or lower CO<sub>2</sub> content than the gas stream originally applied for the absorption.
- 25 19. Use of a composition according to any of claims 1-14 for the removal of CO<sub>2</sub> in stationary plants such as e.g. power plants, or a flue-gas stream in a power plant.

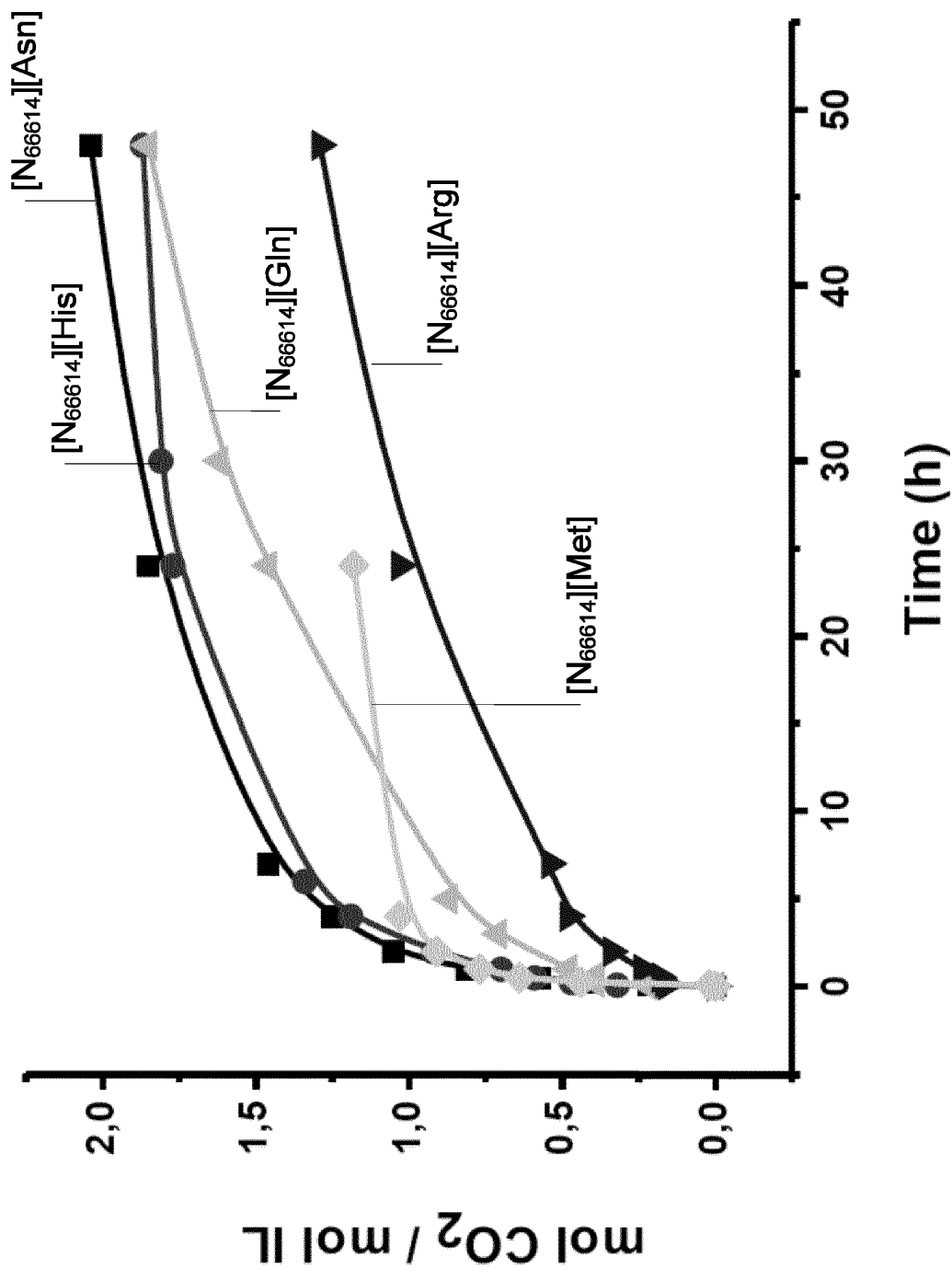


Fig. 1



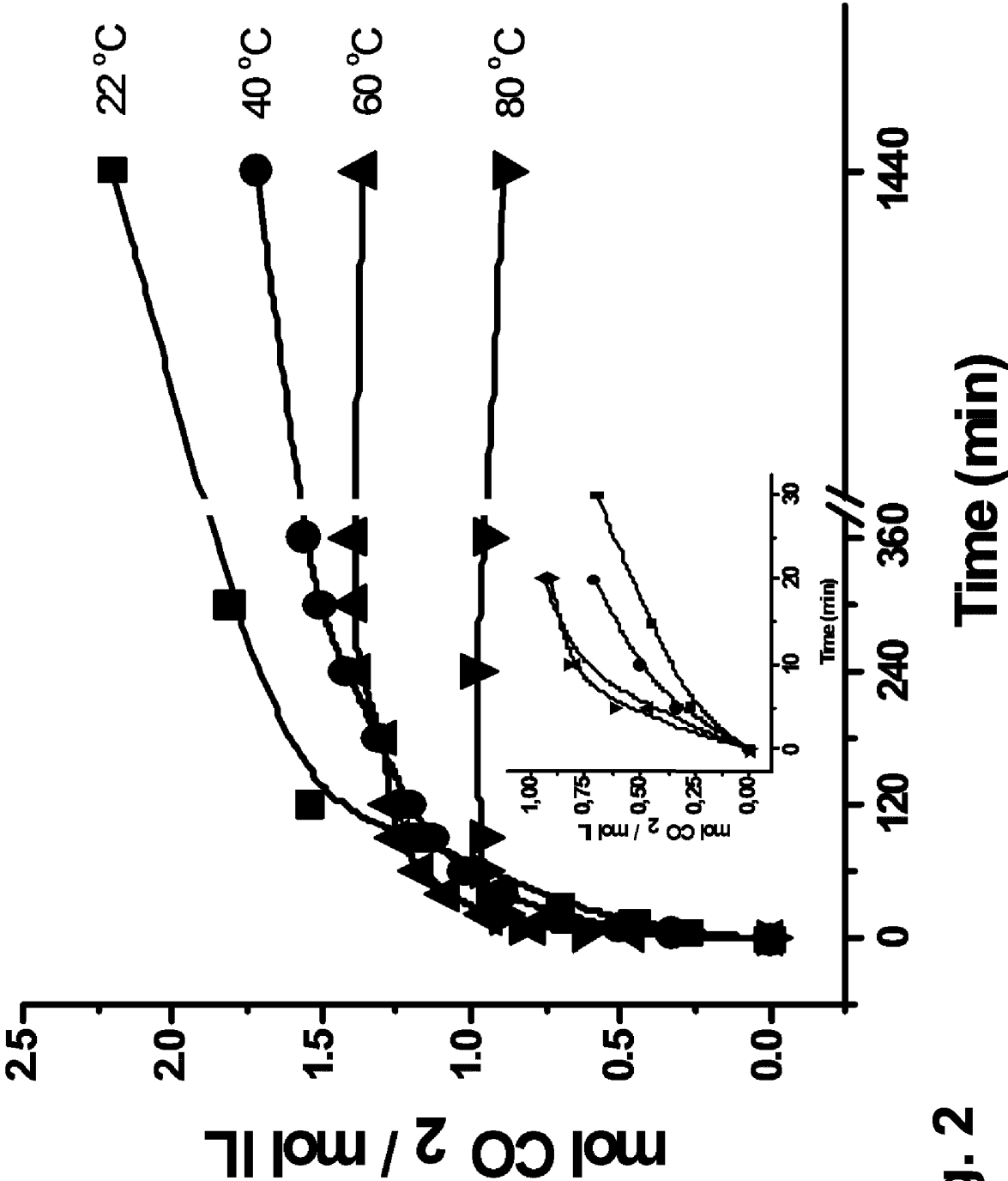
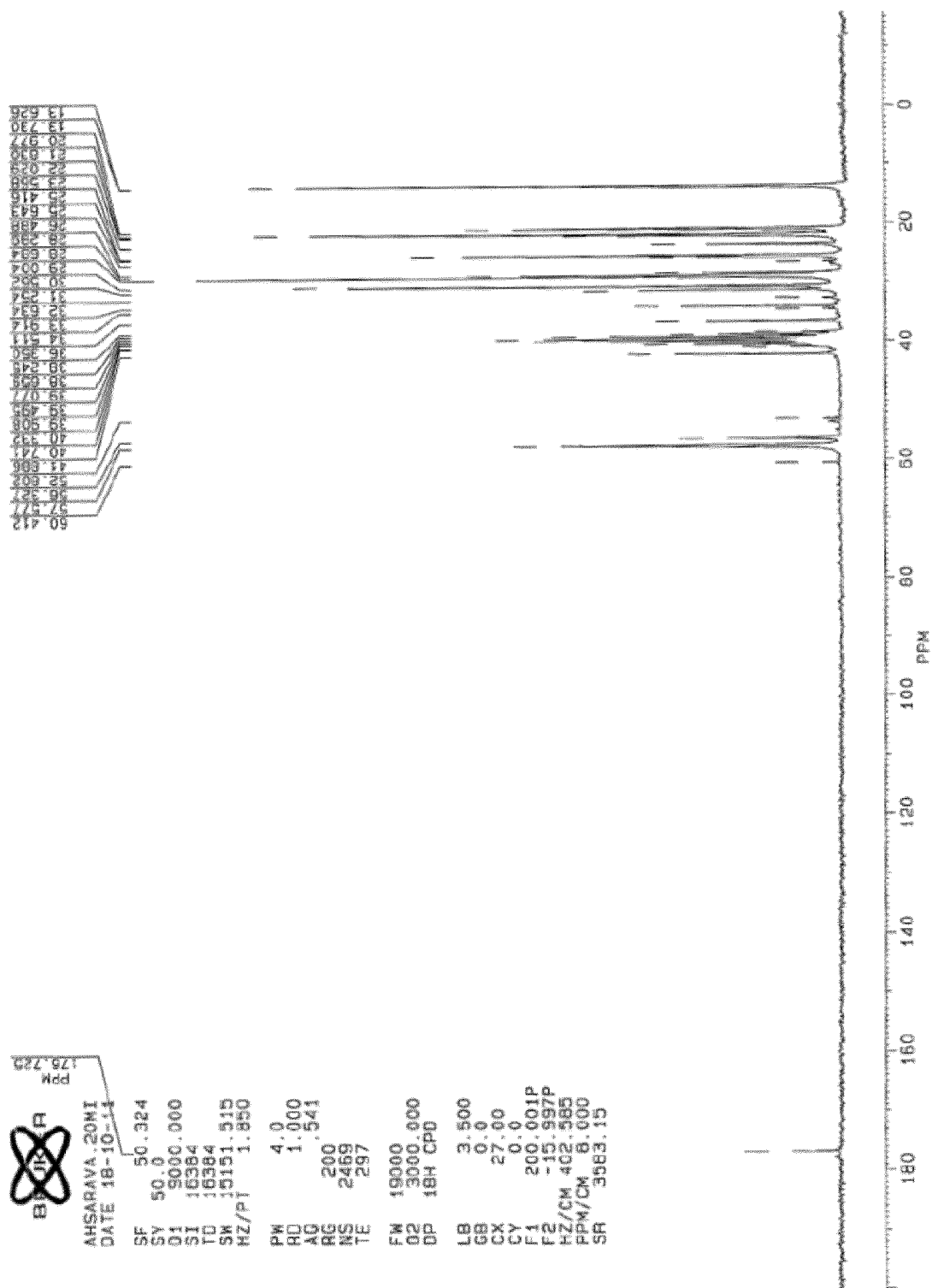


Fig. 2

**3/15**



**Fig. 3a**

4/15

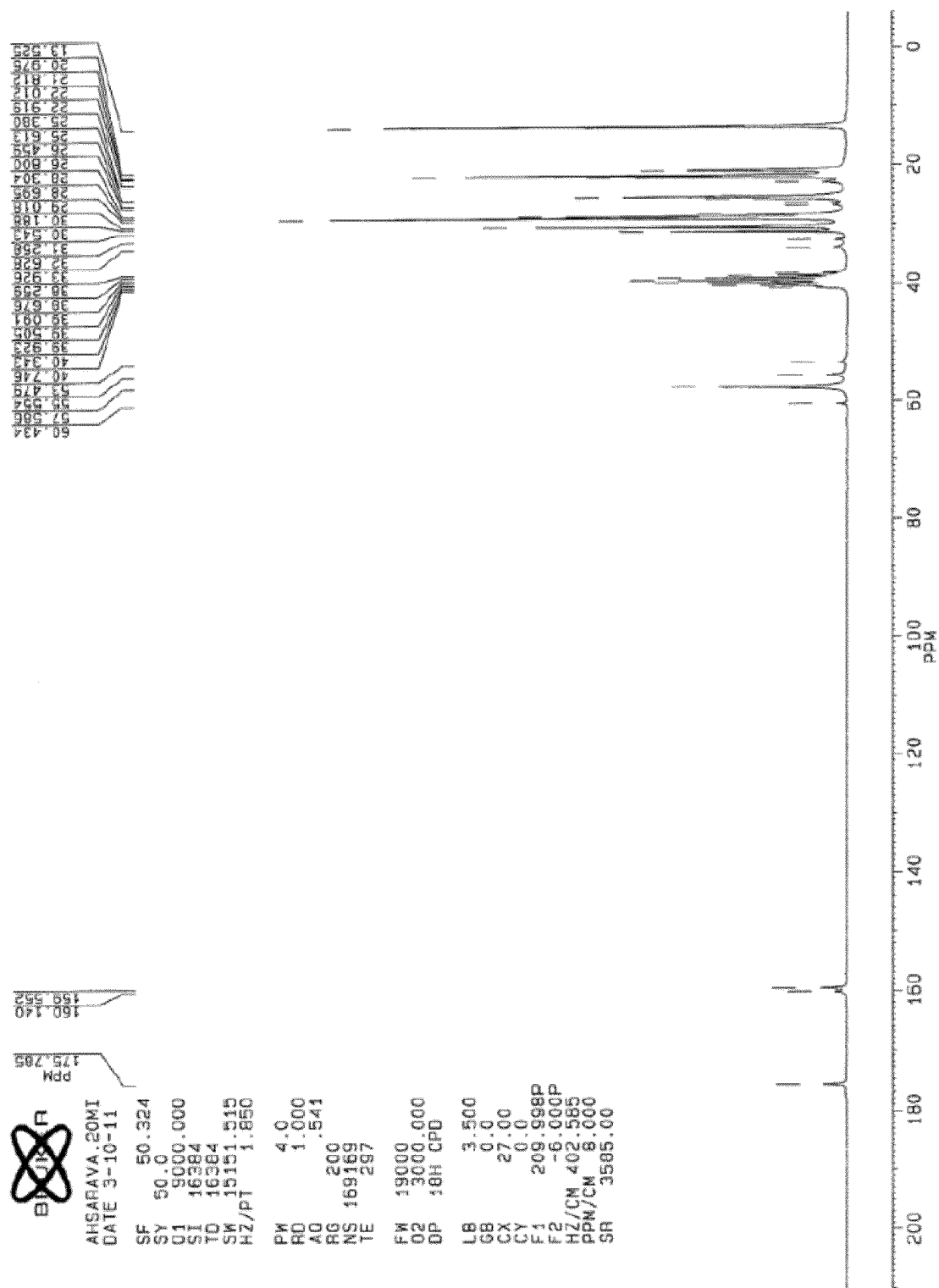


Fig. 3b

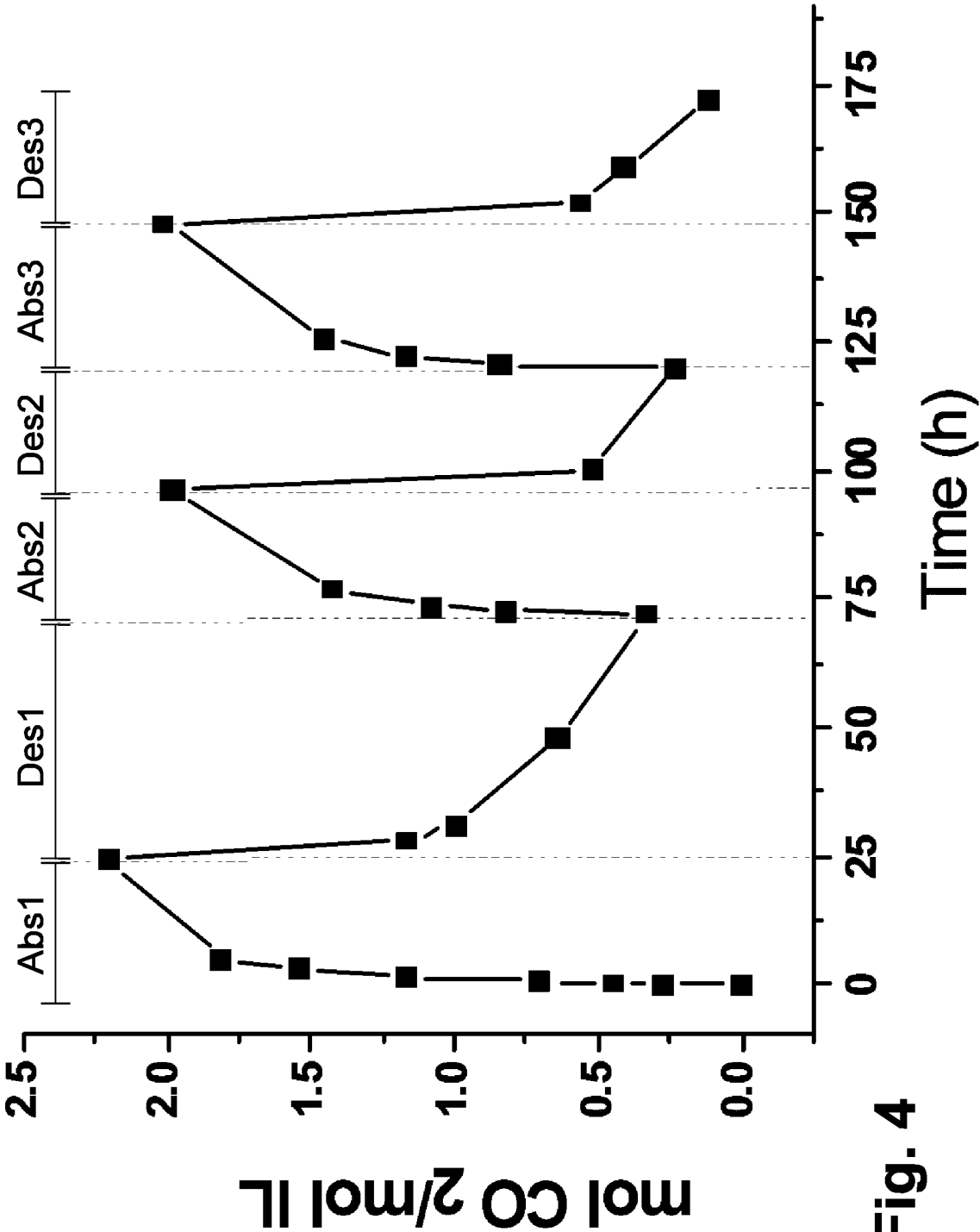


Fig. 4

6/15

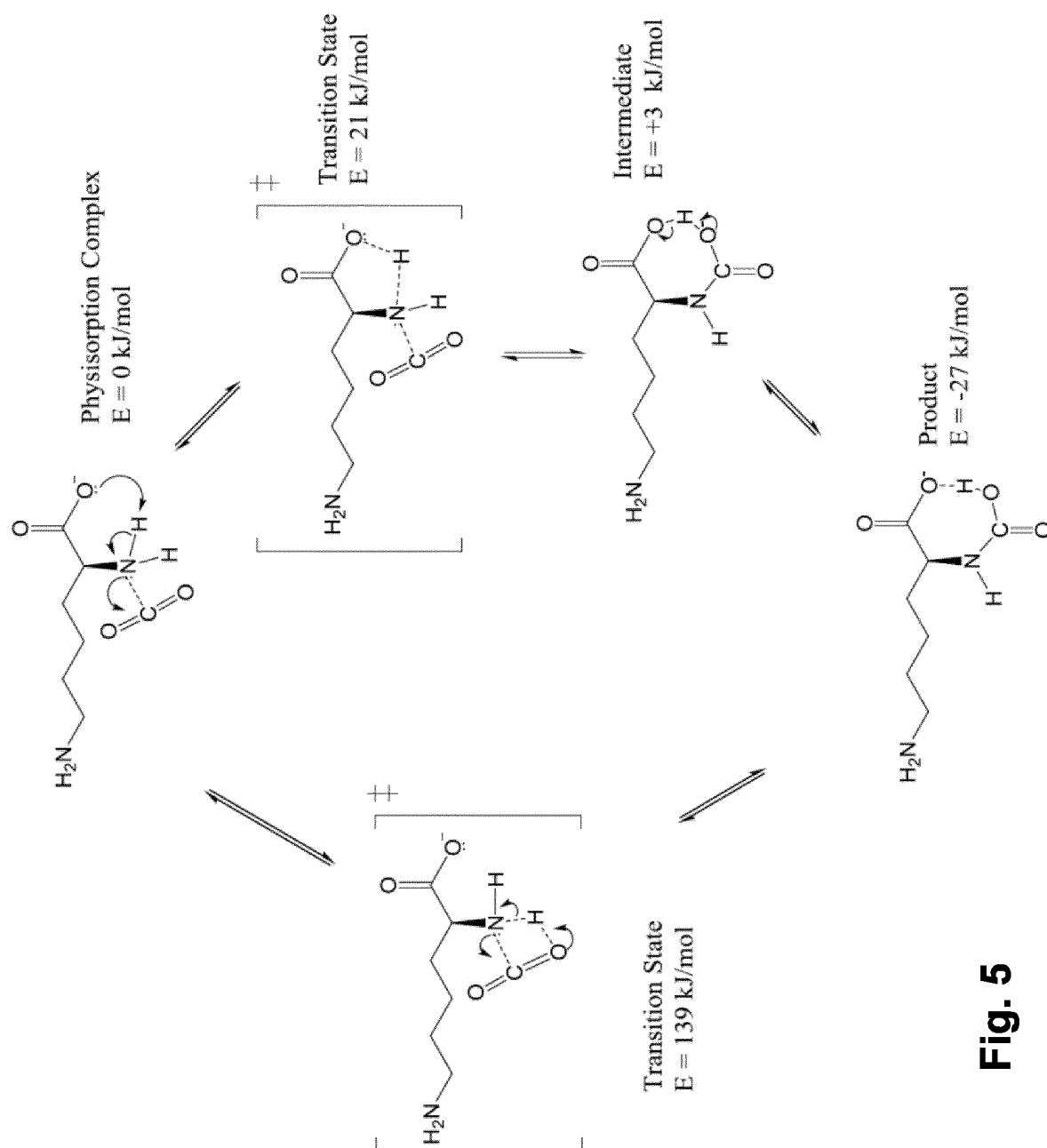


Fig. 5

7/15

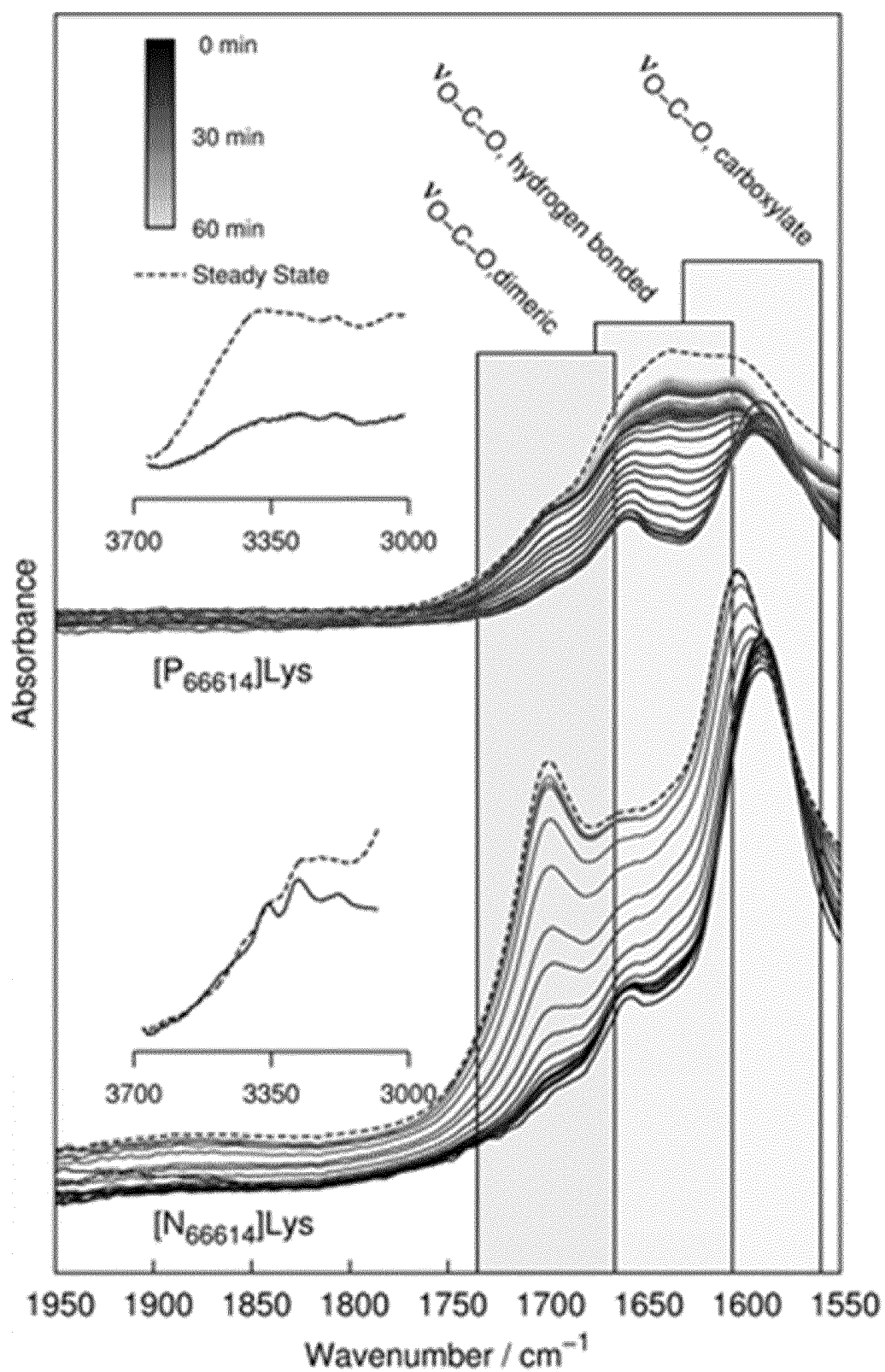


Fig. 6a

8/15

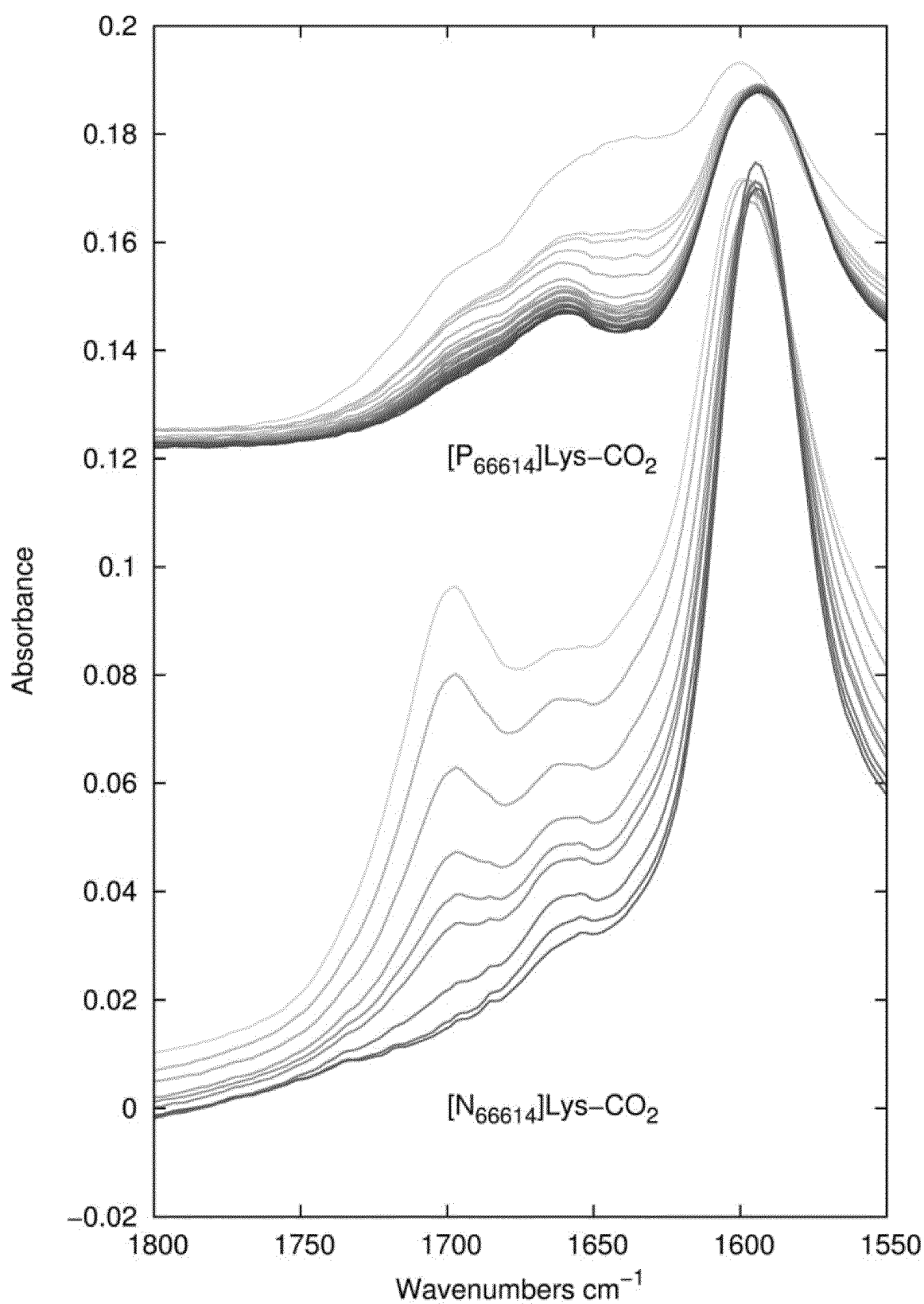


Fig. 6b

9/15

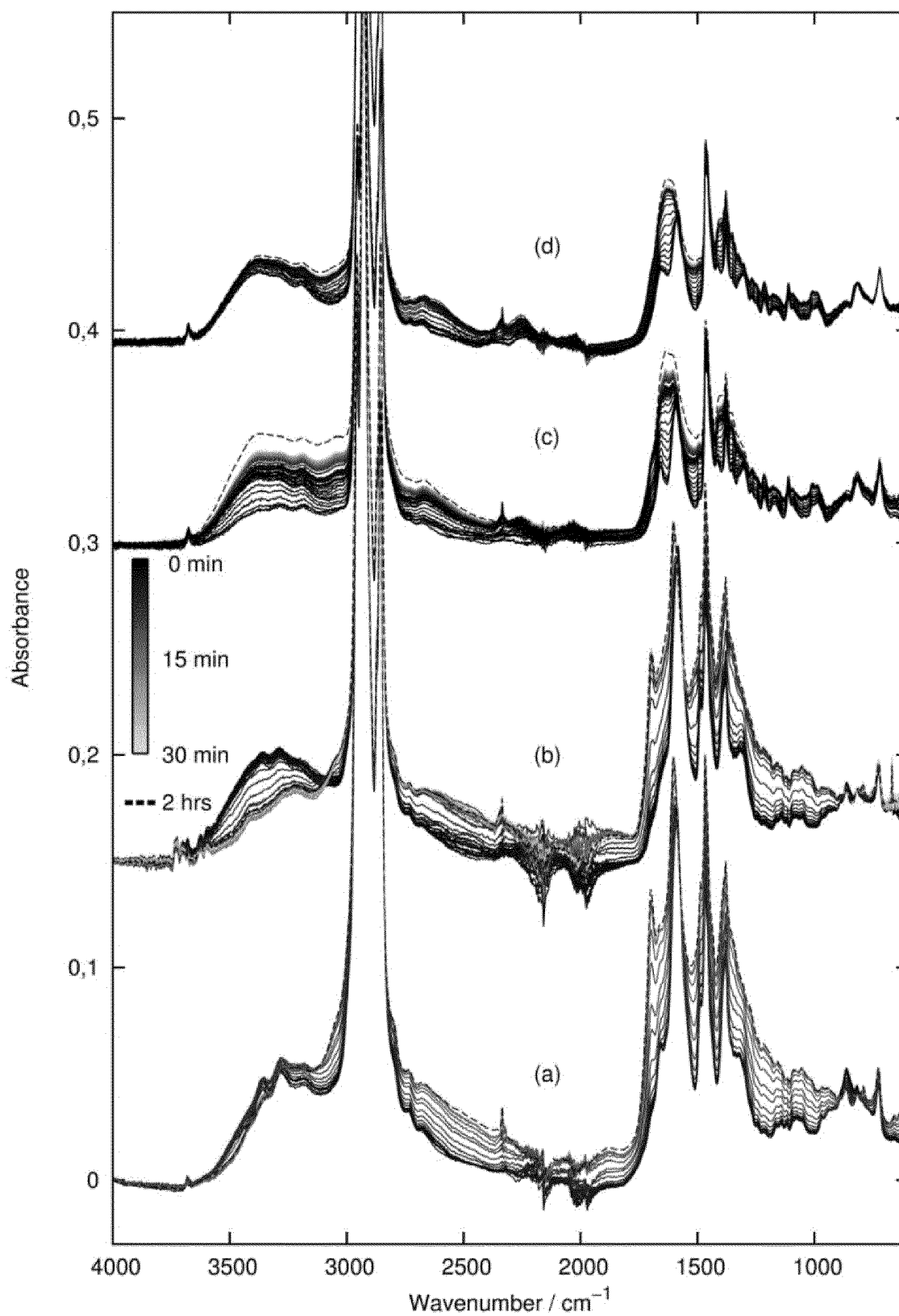


Fig. 7



10/15

	Lysinate		Carboxyl lysinate		Acetic acid dimer	
	Exp	Calc	Exp	Calc	Exp <sup>b</sup>	Calc
$\nu_{C=O, asym}$ carboxylic acid <i>overtone</i>	-	-	1697 (vs) 3408	1702 <sup>c</sup>	1704 (vs)	1701 (s)
$\nu_{C=O, asym}$ carboxylate <i>overtone</i>	1588(vs)	1594 (vs)	- 3220 (w)	1603 (s)	-	-
$\nu_{C=O, asym}$ carboxylate- carboxylic acid <i>overtone</i>			1660- 1645 (s) 3318(w)			
$\delta_{O-H}$ carboxylic acid <i>overtone</i>	-	-	1507 (m) 3025 (w)	1530 (m)	1420 (m)	1405 (m)
$\delta_{N-H, ip}$	844 (m)	803-842 (m)	-	-	-	
$\delta_{N-H,oop}$	1660 (w)	1622-1639 (w)			-	-
$\nu_{N-H, asym}$	3280 (w)	3267(w)	-	-	-	-
$\nu_{N-H, sym}$	3360 (w)	3348(w)	-	-	-	-
$\nu_{N-H}$	-	-	3408 <sup>d</sup>	3446-3453 (vw)	-	-

Fig. 8

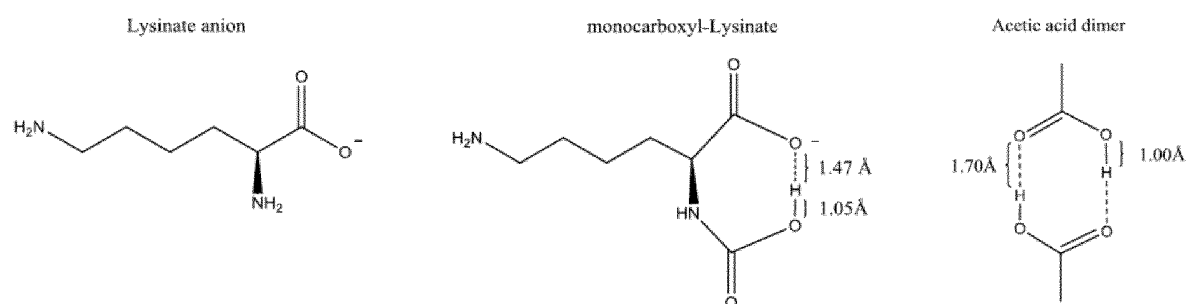


Fig. 9a

11/15

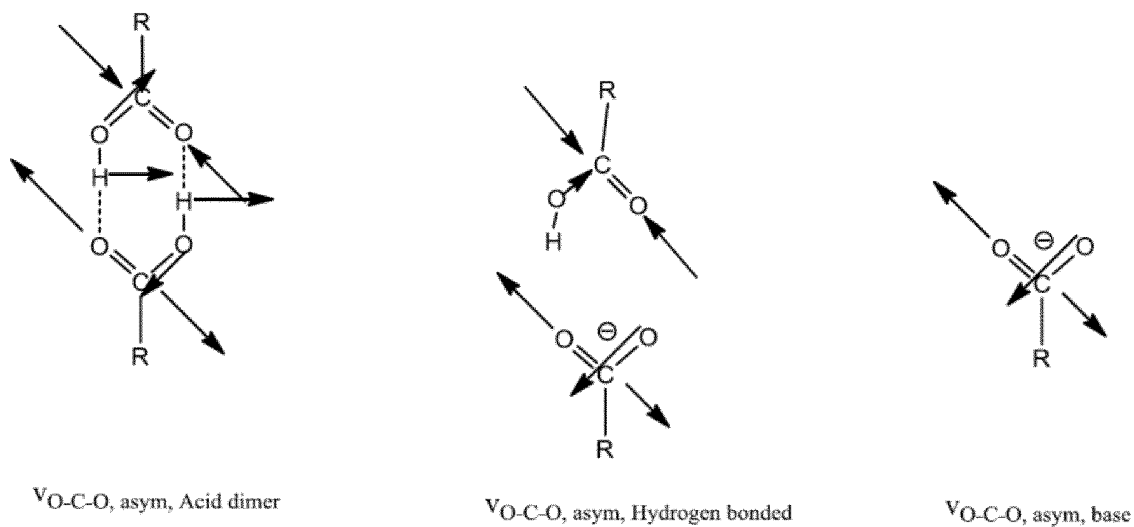


Fig. 9b

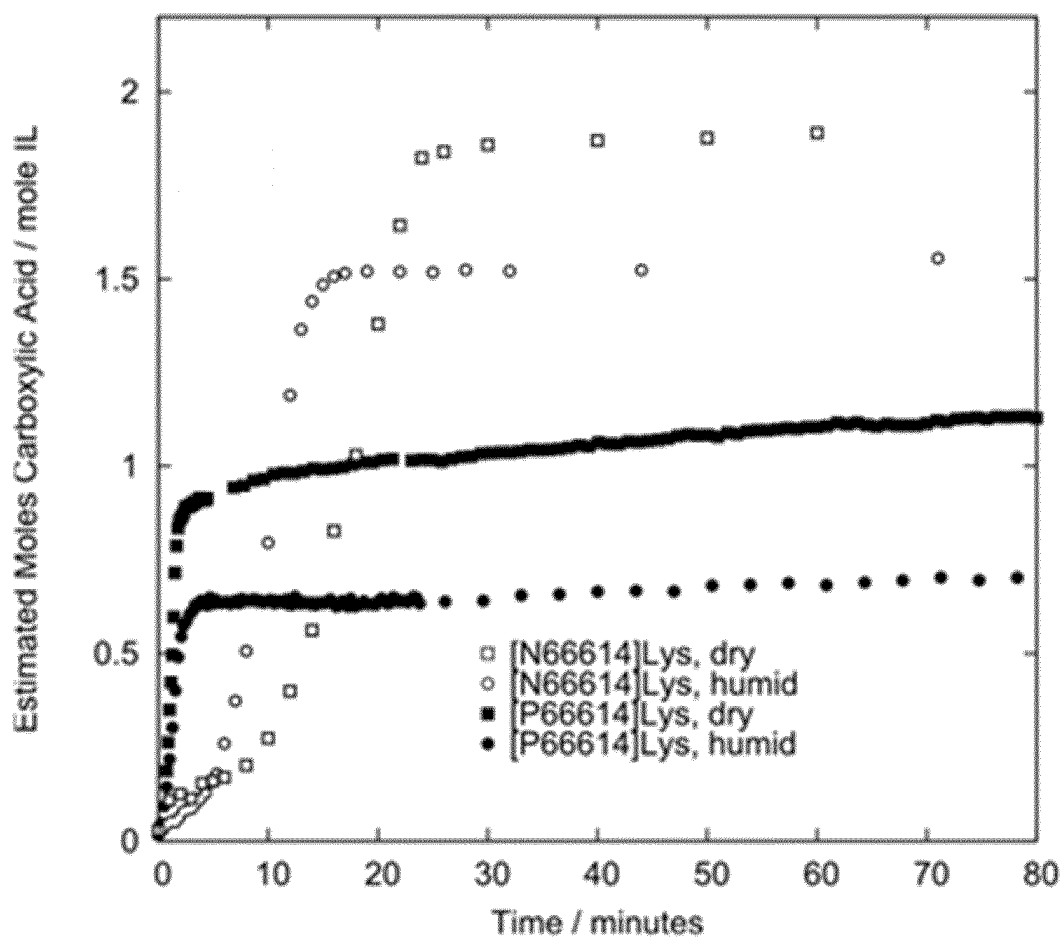


Fig. 10

12/15

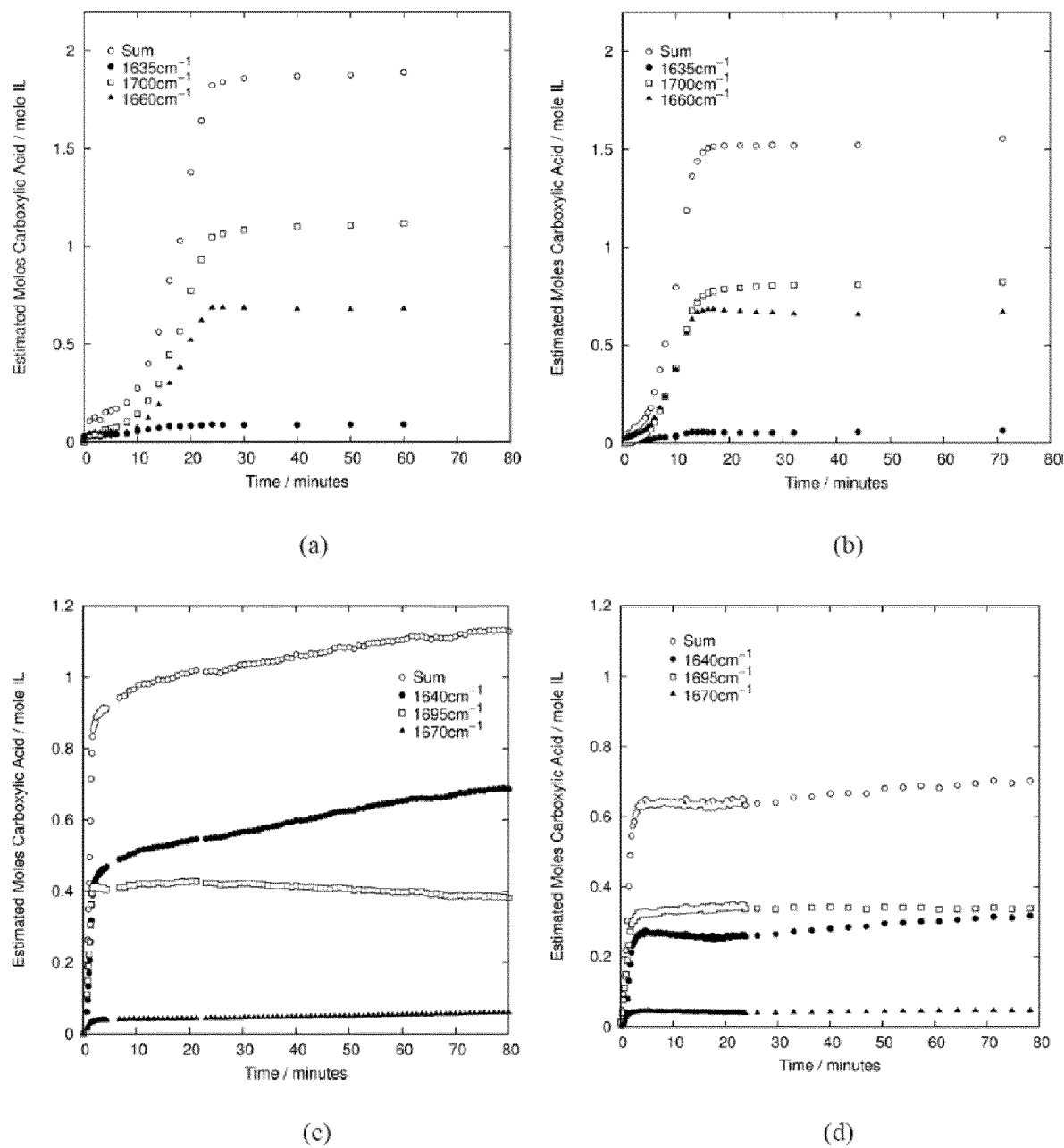
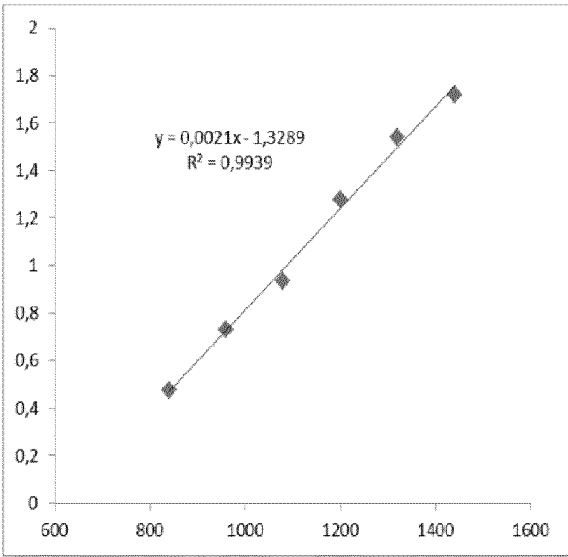
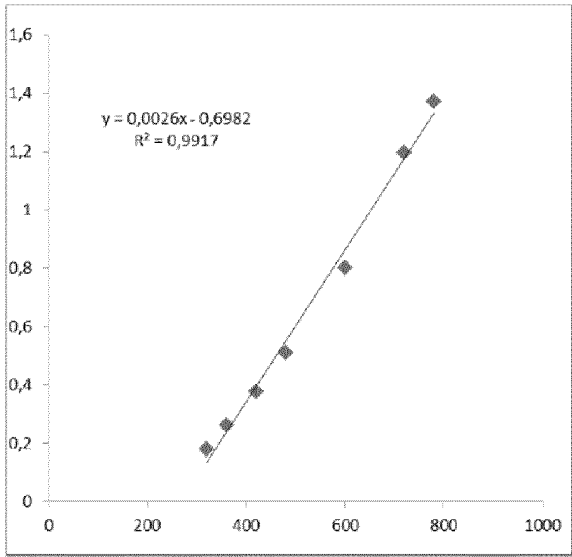


Fig. 11

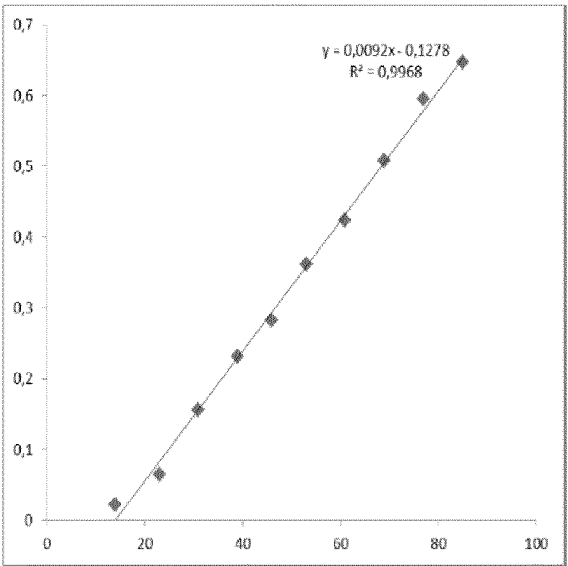
13/15



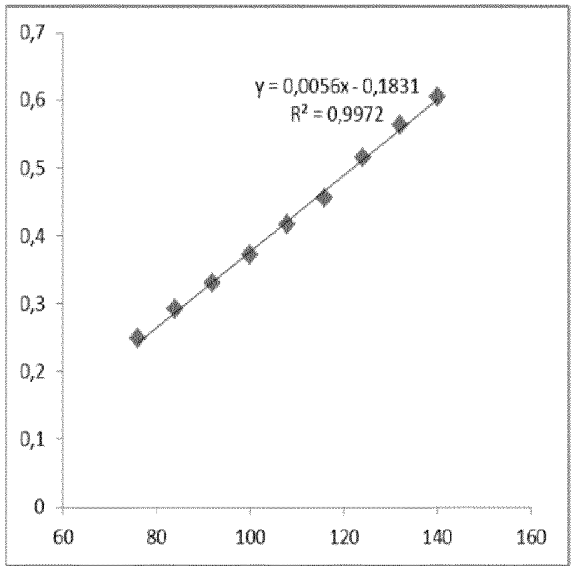
(a)



(b)



(c)



(d)

Fig. 12

14/15

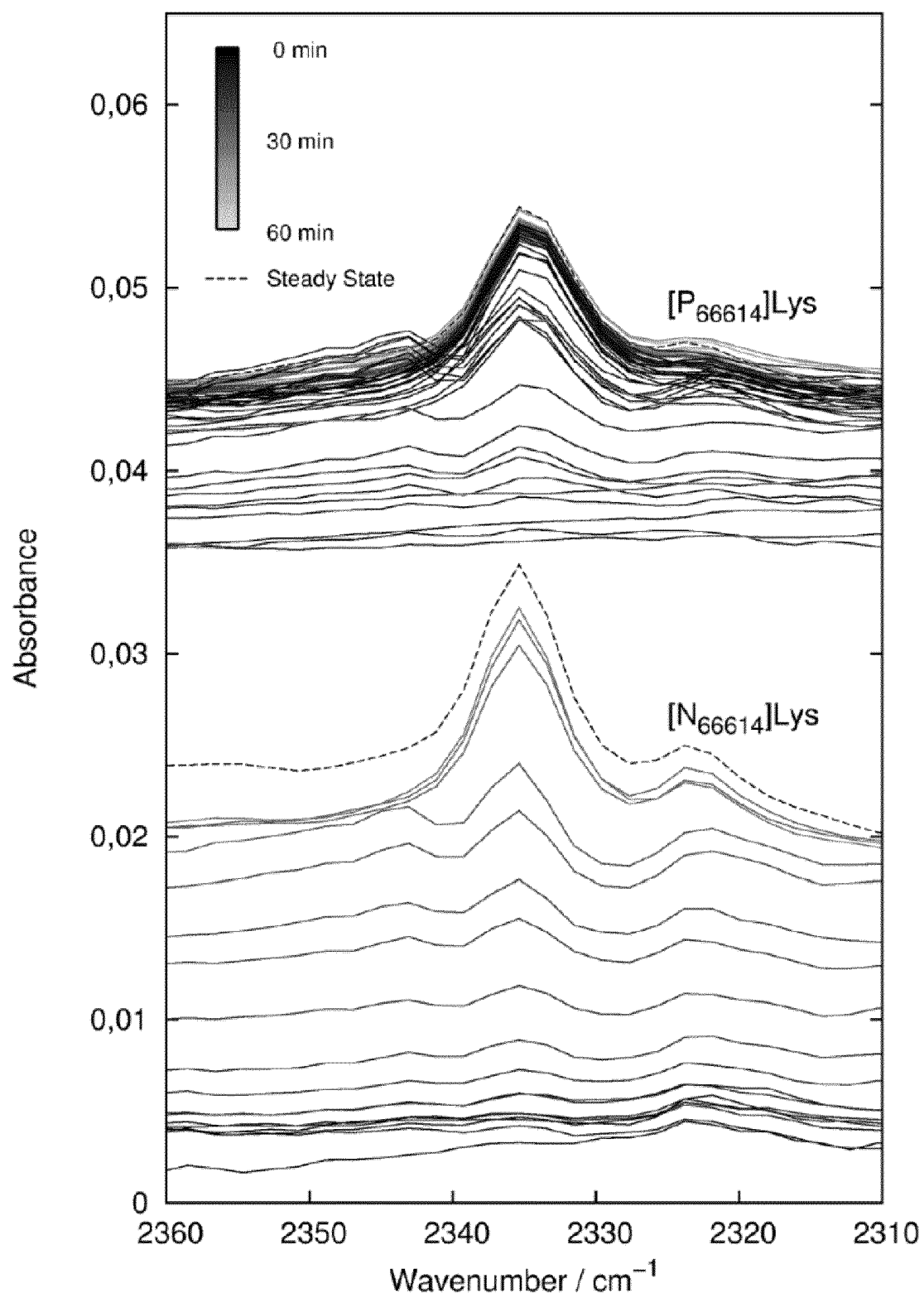


Fig. 13

15/15

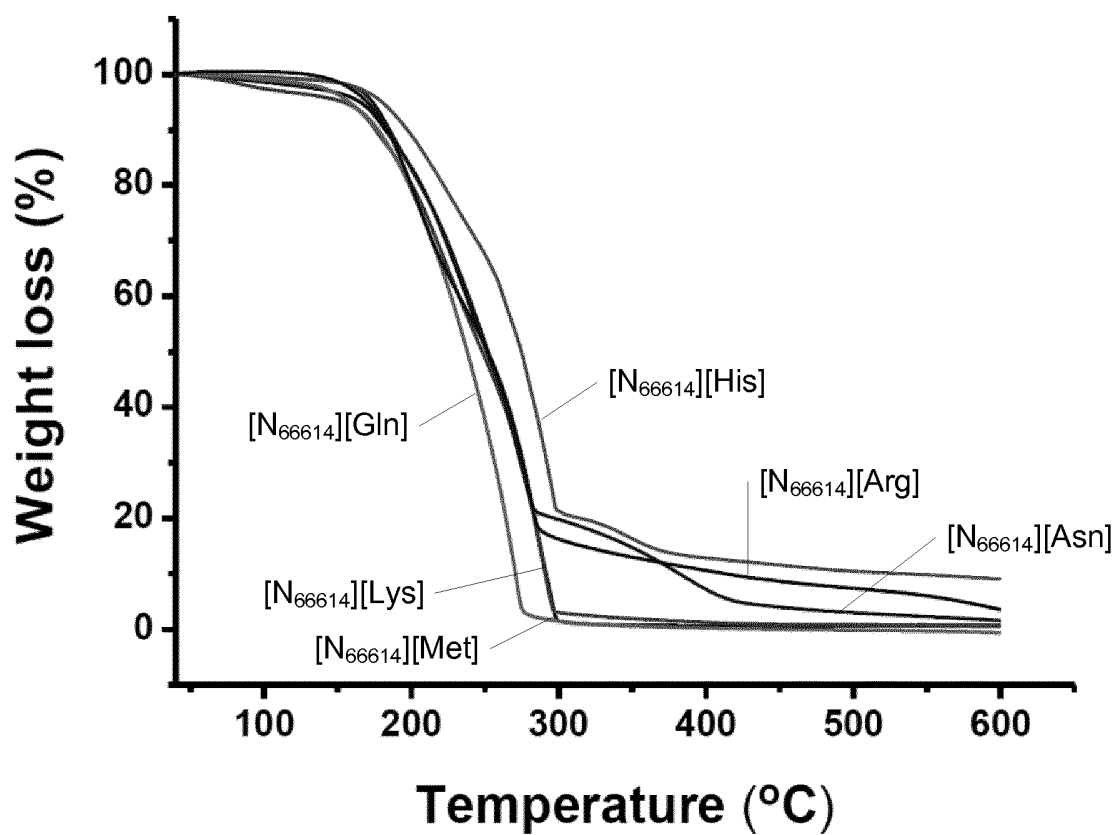


Fig. 14

# INTERNATIONAL SEARCH REPORT

International application No  
PCT/EP2015/050546

A. CLASSIFICATION OF SUBJECT MATTER  
INV. B01D53/14  
ADD.

According to International Patent Classification (IPC) or to both national classification and IPC

## B. FIELDS SEARCHED

Minimum documentation searched (classification system followed by classification symbols)  
B01D

Documentation searched other than minimum documentation to the extent that such documents are included in the fields searched

Electronic data base consulted during the international search (name of data base and, where practicable, search terms used)

EPO-Internal, WPI Data

## C. DOCUMENTS CONSIDERED TO BE RELEVANT

Category*	Citation of document, with indication, where appropriate, of the relevant passages	Relevant to claim No.
Y	BRETT F. GOODRICH ET AL: "Effect of Water and Temperature on Absorption of CO <sub>2</sub> by Amine-Functionalized Anion-Tethered Ionic Liquids", THE JOURNAL OF PHYSICAL CHEMISTRY B, vol. 115, no. 29, 28 July 2011 (2011-07-28), pages 9140-9150, XP055123249, ISSN: 1520-6106, DOI: 10.1021/jp2015534 cited in the application figure 3; table 5  ----- -/--	1-19



Further documents are listed in the continuation of Box C.



See patent family annex.

\* Special categories of cited documents :

"A" document defining the general state of the art which is not considered to be of particular relevance

"E" earlier application or patent but published on or after the international filing date

"L" document which may throw doubts on priority claim(s) or which is cited to establish the publication date of another citation or other special reason (as specified)

"O" document referring to an oral disclosure, use, exhibition or other means

"P" document published prior to the international filing date but later than the priority date claimed

"T" later document published after the international filing date or priority date and not in conflict with the application but cited to understand the principle or theory underlying the invention

"X" document of particular relevance; the claimed invention cannot be considered novel or cannot be considered to involve an inventive step when the document is taken alone

"Y" document of particular relevance; the claimed invention cannot be considered to involve an inventive step when the document is combined with one or more other such documents, such combination being obvious to a person skilled in the art

"&" document member of the same patent family

Date of the actual completion of the international search

12 March 2015

Date of mailing of the international search report

23/03/2015

Name and mailing address of the ISA/

European Patent Office, P.B. 5818 Patentlaan 2  
NL - 2280 HV Rijswijk  
Tel. (+31-70) 340-2040,  
Fax: (+31-70) 340-3016

Authorized officer

Focante, Francesca

## INTERNATIONAL SEARCH REPORT

International application No

PCT/EP2015/050546

C(Continuation). DOCUMENTS CONSIDERED TO BE RELEVANT

Category*	Citation of document, with indication, where appropriate, of the relevant passages	Relevant to claim No.
Y	YING-YING JIANG ET AL: "Tetraalkylammonium amino acids as functionalized ionic liquids of low viscosity", CHEMICAL COMMUNICATIONS, no. 4, 9 November 2007 (2007-11-09), page 505, XP055045225, ISSN: 1359-7345, DOI: 10.1039/b713648j columns 1, 3, 4 -----	1-19
Y	HELENE KOLDING ET AL: "COCapture technologies: Current status and new directions using supported ionic liquid phase (SILP) absorbers", SCIENCE CHINA CHEMISTRY, SP SCIENCE CHINA PRESS, HEIDELBERG, vol. 55, no. 8, 18 July 2012 (2012-07-18), pages 1648-1656, XP035095874, ISSN: 1869-1870, DOI: 10.1007/S11426-012-4683-X sections 1, 2.2.2, 3.2, 4; abstract; table 3 -----	12-14,17
X	US 5 314 852 A (KLATTE FRED [US]) 24 May 1994 (1994-05-24) column 6, lines 26-44; claims 41, 42, 45 -----	1,3,10, 12-14
A	US 2012/204717 A1 (DINNAGE PAUL [US]) 16 August 2012 (2012-08-16) paragraphs [0059] - [0060], [0105], [0107], [0111] - [0122] -----	1-19
A	US 2012/153223 A1 (JEONG SOON KWAN [KR] ET AL) 21 June 2012 (2012-06-21) paragraphs [0055] - [0061]; claim 1; example 1; table 1 -----	1-19
A	JP 2010 214324 A (PETROLEUM ENERGY CENTER FOUND; JX NIPPON OIL & ENERGY CORP) 30 September 2010 (2010-09-30) paragraphs [0015] - [0018] -----	1-19



# INTERNATIONAL SEARCH REPORT

Information on patent family members

International application No

PCT/EP2015/050546

Patent document cited in search report	Publication date	Patent family member(s)	Publication date
US 5314852	A	24-05-1994	NONE
-----			
US 2012204717	A1	16-08-2012	CN 103458994 A 18-12-2013
			CN 103534004 A 22-01-2014
			EP 2673067 A1 18-12-2013
			EP 2673068 A1 18-12-2013
			US 2012204717 A1 16-08-2012
			US 2012204718 A1 16-08-2012
			WO 2012109547 A1 16-08-2012
			WO 2012109550 A1 16-08-2012
-----			
US 2012153223	A1	21-06-2012	KR 20120067046 A 25-06-2012
			US 2012153223 A1 21-06-2012
-----			
JP 2010214324	A	30-09-2010	JP 5378841 B2 25-12-2013
			JP 2010214324 A 30-09-2010
-----			